

UNIVERSIDADE DE LISBOA
FACULDADE DE CIÊNCIAS
DEPARTAMENTO DE BIOLOGIA ANIMAL



**Pharmaceuticals in coastal waters: screening and
environmental risk assessment**

Henrique Vieira Mourato

Mestrado em Biologia da Conservação

Dissertação orientada por:
Doutora Vanessa Fonseca e Doutor Bernardo Duarte

Acknowledgements

I would like to extend my gratitude to my instructors for their support, invaluable guidance, and for the opportunities they provided throughout this academic journey. Their support and commentary have been instrumental in shaping my experience.

I am also thankful to the laboratory research group for their assistance during this project. Their expertise, collaborative spirit, and willingness to share their knowledge were instrumental in the success of this project, and I am very grateful for their contributions.

Furthermore, I extend appreciation to the university for its financial support and for giving me the opportunity to enrol in this project and granting me access to the essential facilities that made this endeavour possible.

Thank you all for your support and contributions.

Abstract

Coastal ecosystems are highly productive and anthropogenically degraded habitats. Compounds like pharmaceuticals or trace metals can be found at high frequencies in estuarine waters and their effects on the ecosystem are not fully understood. Pollution-sensitive phytoplankton, like the diatom *Phaeodactylum tricornerutum*, are essential for ecosystem functioning and have been used in multiple ecotoxicological assessments. Immobilization of *P. tricornerutum* in alginic spheres has been used in environmental monitoring due to their efficacy in pollutant detection and cost-effectiveness. Testing the novel combination of non-invasive bio-optical techniques and the immobilization technique in lab settings may prove useful for daily *in situ* monitoring. Additionally, a creation of a pharmaceutical risk matrix focused on marine algae was created. There was a 100% detection rate for pharmaceuticals in all water samples, with β -blockers and antibiotics being detected most frequently. Antidepressants, β -blockers and antihypertensives exhibited the highest concentrations. β -blockers, antidepressants, antihypertensive and antibiotics reached moderate risk. Tejo estuary exhibited the highest pharmaceutical concentrations. Immobilized *P. tricornerutum* revealed significant photo-physiological discrepancies regarding the Performance Index between water samples. Most correlation coefficients indicated a negative association between pharmaceutical concentrations and photochemical traits, except for Structural and Functional Index of the Non-Photochemical Reactions. Only lead and titanium exhibited significant photo-physiological correlations however, the Pollution Load Index was 0 in all samples. Overall, the study revealed the methodology's effectiveness in pharmaceutical detection while emphasizing the need for ecological regulations.

Keywords: Ecology, Aquatic Systems, Water Quality, Biomonitoring, Photosynthetic Fluorescence

Resumo

Estuários, tal como outras regiões marinhas biologicamente e economicamente importantes, estão mundialmente sob grandes pressões antropogénicas. Entre as principais pressões está a poluição da água, através de múltiplas fontes, incluindo a indústria, a dispersão de águas agrícolas ou urbanas, a aquicultura, a pecuária ou a descarga de estações de tratamento de águas residuais. Estas descargas são o principal ponto de entrada para uma vasta gama de poluentes, incluindo nutrientes, compostos orgânicos e outros contaminantes químicos emergentes. Apesar de se estar a introduzir uma quantidade relativamente baixa por composto (ca. ng/L), a descarga contínua pode levar a concentrações crescentes dos mesmos originando por sua vez efeitos desconhecidos a longo prazo. Apesar dos fármacos serem principalmente concebidos para uso humano ou veterinário – através de vias metabólicas conhecidas e em doses baixas –, espécies não-alvo com elevado número de vias metabólicas evolutivamente conservadas podem sofrer efeitos desconhecidos ou imprevistos. Dado que o fitoplâncton é uma das principais fontes de energia primária para a maioria dos ecossistemas aquáticos e é sensível a poluentes, estes organismos, e em particular a diatomácea *Phaeodactylum tricornutum*, têm sido objeto de vários estudos ecotoxicológicos. A sensibilidade da espécie às alterações físicas e químicas torna-a um excelente bioindicador para avaliar a qualidade da água. A imobilização de células de *P. tricornutum* em esferas de alginato foi escolhida como uma abordagem potencialmente valiosa para a monitorização ambiental, dada a sua relação custo-eficácia na deteção de poluentes. Já a capacidade desta abordagem para detetar fármacos em concentrações ambientais ainda não foi avaliada. Dado que a fotoquímica celular sofre alterações rápidas sob stresse, métodos óticos podem ser usados para detetar as mesmas, permitindo medições diárias *in situ* e, portanto, reduzindo a carga de trabalho laboratorial necessária para a obtenção de dados. O principal objetivo deste projeto foi avaliar a eficácia de células imobilizadas de *P. tricornutum* como biomonitores de contaminação de água em amostras ambientais através da aplicação de medidas bio-óticas não invasivas sobre os principais parâmetros fotofisiológicos e compará-los com a pressão antropogénica que contaminantes clássicos (metais) e emergentes (fármacos) exercem.

Foram selecionados seis pontos de amostragem, abrangendo quatro estuários ao longo da costa Portuguesa (Douro, Tejo, Sado, Mira), juntamente com um local costeiro adjacente ao estuário do Tejo (Cabo Raso). O “Pollution Load index” (PLI) foi usado como modelo matemático para resumir as concentrações de metais. O potencial risco ecológico das amostras de água foi analisado através do quociente de risco (RQ), utilizando as concentrações ambientais medidas (MEC) e as concentrações sem efeito previsto (PNEC). A avaliação da toxicidade de fármacos em mistura foi baseada na metodologia proposta por Backhaus e Faust, 2012 onde os quocientes de risco (RQ) são obtidos através do ratio entre concentrações detetadas e a concentração máxima sem efeitos previstos. Por sua vez a utilização de dados relativos à toxicidade de cada composto consiste na soma dos quocientes de risco (RQ) para fármacos com base na concentração mais baixa capaz de induzir efeitos tóxicos. A análise de componentes principais (PCA) foi aplicada aos dados de caracterização química ambiental das águas recolhidas, para avaliar padrões de contaminação espacial e visualizar possíveis relações entre contaminantes. A análise canónica de coordenadas principais (CAP), foi realizada a partir dos dados fotobiológicos e utilizada para identificar dissimilaridades entre parâmetros fisiológicos e determinar o ponto temporal com maior separação de grupos para caracterizar o modelo fotobiológico e avaliar as respostas. Os testes Kruskal-Wallis foram utilizados para determinar diferenças significativas entre variáveis bióticas e abióticas e os coeficientes de correlação de Spearman para determinar possíveis

correlações entre variáveis fisiológicas e concentrações ambientais. A presença de poluentes emergentes foi observada em todas as 44 amostras, e dos 69 compostos testados, foram detetados 23. Dois grupos terapêuticos tiveram frequência de deteção acima de 95%: β -bloqueadores e antibióticos. Os antibióticos foram o grupo terapêutico com a maior variedade de compostos detetados, sendo que a maioria em concentrações relativamente baixas (<8 ng/L). Os antihipertensivos, β -bloqueadores e os antidepressivos foram as classes com maiores concentrações em todas as amostras. As amostras do estuário do Tejo (Tj1 e Tj2) foram as amostras com concentrações medianas de fármacos mais elevadas (1898,88 ng/L e 1198,2 ng/L, respetivamente). Quatro compostos – Bisoprolol, Irbesartan, Losartan e Venlafaxina – foram detetados em níveis consideravelmente superiores aos relatados em 2021.

As concentrações de metais detetadas foram baixas (<0,55 mg/L) e foi obtido um PLI = 0 para todas as amostras. Os dois primeiros componentes da PCA explicaram 62.6% da variação nos dados ambientais (metais e fármacos). Dos 23 fármacos detetados tres antidepressivos e dois antihipertensivos, foram categorizados como risco moderado, sete compostos foram classificados como baixo risco e onze indicam nenhum risco ambiental. Avaliando por pontos de amostragem, apenas os pontos dentro do tejo (Tj1 e Tj2) atingiram a categoria de elevado risco ecológico requerendo implementação de medidas de regulação.

Os RQ obtidos diferem de outros estudos que consideram concentrações em toda a Europa. Diclofenac, Carbamazepin e Venlafaxina são considerados compostos de alto risco na Europa, no entanto as concentrações detetadas pertencem a uma faixa inferior (risco moderado a baixo). As curvas de Kautsky obtidas da exposição das diatomáceas demonstram decréscimo em certas fases durante o período de incubação. A análise CAP determinou que às 24h de exposição das amostras foi obtida a eficiência de classificação máxima de 91,1%. Os parâmetros fotofisiológicos derivados dos testes de fluorescência de clorofila (OJIP) realizados nas diatomáceas apresentaram variações distintas e únicas entre as diatomáceas expostas às diferentes amostras. Existem algumas correlações entre os fármacos e as características fotoquímicas das diatomáceas, sendo que a maioria, fluxo de energia de transporte relativo e absoluto (ET/RC e ET/(%)), o índice estrutural e funcional (SFI), e o índice de desempenho (PI) estão negativamente correlacionadas com o aumento da concentração de fármacos. O índice estrutural e funcional para as reações não fotoquímicas (SFI(NPQ)) é o único que está positivamente correlacionado. Apenas os metais, chumbo e titânio tiveram alguma correlação com a fotofisiologia.

Embora as amostras recolhidas no estuário do Tejo (Tj1 e Tj2) demonstrem níveis de poluição semelhantes com um RQ superior a 1, estas apresentam características fotoquímicas significativamente diferentes entre si. Uma vez que é difícil identificar qual o composto ou combinação dos mesmos que é responsável por uma determinada resposta metabólica é importante realçar que estes poluentes exercem claros sinais de stresse às diatomáceas, tal como fariam em condições ambientais reais.

Os resultados evidenciam que é possível realizar uma análise diária custo-efetiva contínua recorrendo a esta metodologia. Para manter um ecossistema estuarino ou costeiro estável e biodiverso, monitorizar e compreender o efeito que poluentes tais como fármacos ou metais podem ter na fauna e flora é fundamental. A desestabilização das populações de fitoplâncton através da contaminação da água pode ter efeitos em cascata em toda a rede trófica. Além disso, a biomagnificação de fármacos ou de metabólitos pode afetar negativamente a biodiversidade local. A sustentabilidade a longo prazo está intrinsecamente relacionada com a qualidade da água pelo que a sua monitorização é crucial para a deteção de novas tendências de poluição. Só

acompanhando a qualidade da água será possível a rápida implementação de medidas ambientais adequadas, por forma a garantir a capacidade natural do habitat.

Palavra-chave: Ecologia, Sistemas Aquáticos, Qualidade da Água, Monitorização Ambiental, Florescência Fotossintética

Index

ACKNOWLEDGEMENTS	II
TABLE LIST	VIII
FIGURE LIST	VIII
SUPPLEMENT LIST	IX
1. INTRODUCTION	1
2. MATERIALS AND METHODS	3
2.1. STUDY AREA AND SAMPLE COLLECTION	3
2.2. WATER CHEMICAL ANALYSIS	5
2.3. EXPERIMENTAL PROCEDURE	5
2.4. DATA ANALYSIS	6
3. RESULTS	8
3.1 WATER CHEMICAL CHARACTERIZATION AND RISK ASSESSMENT	8
3.2 IMMOBILIZED DIATOM EXPOSURE TRIALS	15
4. DISCUSSION	19
5. CONCLUSION	22
6. REFERENCES	X
7. SUPPLEMENTS	XXII

Table List

Table 1. Water sampling sites coordinates, mean sample salinity \pm standard deviation and number of samples collected (N).	3
Table 2. Geomorphologic and Hydrologic characteristics of sampled estuarine systems - Douro, Tejo, Sado, and Mira, along with details on the resident population and wastewater treatment facilities in the surrounding municipalities adapted from (Duarte et al., 2023).	4
Table 3. Chlorophyll fast induction kinetics derived parameters adapted from Duarte et al., (2021).	6
Table 4. Summary of the 23 pharmaceuticals from 7 therapeutic groups detected (N= 26 water samples). Includes detection frequency (%), median, minimum, average (Standard Error), and maximum concentrations (ng/L ⁻¹). (< LOQ = below limits of quantification).	11

Figure List

Figure 1. Water collection sites in estuaries along the Portuguese coast, namely in Douro (Do), Tejo (Beirolos-Tj1, Mutela-Tj2 and adjacent nearshore area Cabo Raso-CR) Sado (Sa) and Mira (Mi).	3
Figure 2. Pharmaceutical concentration in water samples by therapeutic group (ng/L) across all sampling sites (Do-Douro Estuary N=5 ; CR – Cabo Raso N=3 ; Tj1 and Tj2 – Tejo Estuary Sampling Site 1 and 2, N=5 and N=3 respectively; Sa – Sado Estuary N=5; Mi – Mira Estuary N=5) (letters denote significant differences at $p < 0.05$) by therapeutic group.	9
Figure 3. Trace metal concentrations (mg/L) across all sampling sites sites (Do-Douro Estuary; CR – Cabo Raso; Tj1 and Tj2 – Tejo Estuary Sampling Site 1 and 2 respectively; Sa – Sado Estuary; Mi – Mira Estuary) (N=3 per site, letters denote significant differences at $p < 0.05$)	12
Figure 4. Principal component analysis (PCA) of Pharmaceuticals and metal concentrations found at each site. (Do – Douro, CR – Cabo Raso, Tj1 – Tejo 1 Beirolos, Tj2 – Tejo 2 Mutela and Mi – Mira)	13
Figure 5. Risk quotients (RQ) of the maximum concentration detected for each pharmaceutical (A), therapeutic Group (B), and each sampled site (C).	14
Figure 6. Variable fluorescence curves, following chlorophyll a fluorescence induction curves of <i>Phaeodactylum tricornutum</i> cultures from all sampled sites over 6-day period (Do – Douro, CR – Cabo Raso, Tj1 – Tejo 1 Beirolos, Tj2 – Tejo 2 Mutela and Mi – Mira) (average, N=3 per site)	15
Figure 7. Canonical analysis of principal coordinates (CAP) classification accuracy between sites at each exposure timepoint (up to 144h) and model overall accuracy (Total) .	16
Figure 8. OJIP-derived physiological parameters ("PI"-Performance Index, "ABS/RC"-Absorbed energy flux per reaction center, "TRo/RC"-Trapped energy flux per reaction center, "TR(%)"-Relative Trapped energy flux normalized towards the absorbed energy flux (TRo/RC)/(ABS/RC) x 100, "ETo/RC"-Transported energy flux per reaction center, "ET(%)"-Relative Transported energy flux normalized towards the trapped energy flux (ETo/RC)/(TRo/RC) x 100, "DIo/RC"-Dissipated energy flux per reaction center, "DI(%)"-Relative Dissipated energy flux normalized towards the absorbed energy flux (DIo/RC)/(ABS/RC) x 100, "SFI"-Structural and Functional Index of the Photochemical Reactions,"SFI (NPQ)" - Structural and Functional Index of the Non-Photochemical Reactions.), Different letters denote significant differences at $p < 0.05$	17
Figure 9. Spearman correlation coefficients (N=5) correlograms between photo-physiological parameters and pharmaceutical concentrations (A), metal concentrations (B) and the RQ (therapeutic group) (C). Positive correlations are represented in green and negative correlations in magenta. Only significant ($p < 0.05$) correlations are displayed. "AAP"-Acetaminophen, "AT"-Atenolol, "AZM"-Azithromycin, "BIS"-Bisoprolol, "BZF"-	

Bezafibrate, "CBZ"-Carbamazepine, "CIP"-Ciprofloxacin, "CIT"-Citalopram, "DCF"-Diclofenac, "DOX"-Doxycycline, "ESC"-Escitalopram, "FLU"-Flumequine, "HALZ"-Alpha-Hydroxyalprazolam, "IND"-Indapamide, "IRB"-Irbesartan, "LZP"-Lorazepam, "LOS"-Losartan "PRO"-Propranolol, "SER"-Sertraline, "SMX"-Sulfamethoxazole, "SP"-Sulfapyridine, "TMP"-Trimethoprim, "VEN"-Venlafaxine,"PI"-Performance Index, "ABS/RC"-Absorbed energy flux per reaction center, "TRo/RC"-Trapped energy flux per reaction center, "TR(%)"-Relative Trapped energy flux normalized towards the absorbed energy flux $(TRo/RC)/(ABS/RC) \times 100$, "ETo/RC"-Transported energy flux per reaction center, "ET(%)"-Relative Transported energy flux normalized towards the trapped energy flux $(ETo/RC)/(TRo/RC) \times 100$, "DIo/RC"-Dissipated energy flux per reaction center, "DI(%)"-Relative Dissipated energy flux normalized towards the absorbed energy flux $(DIo/RC)/(ABS/RC) \times 100$, "SFI"-Structural and Functional Index of the Photochemical Reactions,"SFI (NPQ)"-Structural and Functional Index of the Non-Photochemical Reactions.

18

Supplement List

Table supplement 1. List of the 69 compounds screened	XXII
Table supplement 2. Limits of detection (LOD) of the 23 pharmaceuticals detected	XXIV

Abreviation list

Sites

Do - Douro
 CR - Cabo Raso
 TJ1 - Tejo site 1 (Beirolas)
 TJ2 - Tejo site 2 (Mutela)
 Sa - Sado
 Mi - Mira

Terms

ABS/RC - Absorbed energy flux per reaction center
 AF - Assessment Factor
 CAP - Canonical Analysis Of Principal Coordinates
 DIo/RC - Dissipated energy flux per reaction center
 EC50 - Half Maximal Effective Concentration
 ETo/RC - Transported energy flux per reaction center
 Fo - Basal fluorescence (at t=0)
 IC50 - Half Maximal Inhibitory Concentration
 LOD - Limit Of Detection
 LOQ - Limit Of Quantification
 MAC - Maximum Allowable Concentration
 MEC - Measured Environmental Concentration
 NSAID - Nonsteroidal anti-inflammatory drug
 OJIP - Chlorophyll fluorescence induction curve
 PCA - Principal Component Analysis
 PEC - Predicted Effect Concentration
 PI - Performance Index
 PLI - Pollution Load Index
 PNEC - Predicted No Effect Concentration

QA - Quinone A
ROS - Reactive Oxygen Species
RQ - Risk Quotient
SFI(NPQ) - Structural and Functional Index of the Non-Photochemical Reactions
SFI - Structural and Functional Index of the Photochemical Reactions
STU - Sum of Toxic Units

Pharmaceuticals

AAP - Acetaminophen
AT - Atenolol
AZM - Azithromycin
BIS - Bisoprolol
BZF - Bezafibrate
CBZ - Carbamazepine
CIP - Ciprofloxacin
CIT - Citalopram
DCF - Diclofenac
DOX - Doxycycline
ESC - Escitalopram
FLU - Flumequine
HALZ - Alpha-Hydroxyalprazolam
IND - Indapamide
IRB - Irbesartan
LZP - Lorazepam
LOS - Losartan
PRO - Propranolol
SER - Sertraline
SMX - Sulfamethoxazole
SP - Sulfapyridine
TMP - Trimethoprim
VEN - Venlafaxin

1. Introduction

Worldwide, coastal water ecosystems, including estuaries, are among the most productive but also more anthropogenically degraded habitats (Lytle & Lytle, 2001; Vasconcelos et al., 2007). These systems are economically important as they play a critical role as a nursery or feeding grounds for various birds, fish, and invertebrates who rely on high prey availability, refuge from predators, and the overall favourable conditions these habitats provide to complete their life cycles (Able, 2005; Beck et al., 2001; Gillanders et al., 2003). Other species of microorganisms, such as algae and intertidal vegetation provide ecosystem services such as water filtration due to their ability to biodegrade pollutants and remove excess nutrients from the water column (D'Alessio et al., 2015). This natural remediation process improves water quality and influences human exposure to emerging and legacy pollutants (Pal et al., 2014). However, it's not possible to fully degrade all contaminants, and through biomagnification along the trophic webs, these pollutants can reach humans on top of the food chain (Ceschin et al., 2021). Multiple studies and legislation recognize that the protection of these systems is not only biologically relevant but paramount in sustaining multiple ecosystem services, among which are stocks of economically valuable species and public health (Beck et al., 2001; Ceschin et al., 2021; Lenanton & Potter, 1987; Levin et al., 2001; Vasconcelos et al., 2007).

However, estuaries and other biological and economically important marine regions are under high anthropogenic pressures globally: as human populations continue to grow nearshore, so do the pressures exerted on their structure and function, since drivers of population growth – such as resource exploitation or increased energy consumption –, are connected to local and global declining environmental conditions (WOA, 2021). Among the main pressures is water pollution, via multiple sources including industry, agricultural or urban runoff, aquaculture, husbandry, or discharge from wastewater treatment plants (WWTP). These discharges are the main entry point for a wide range of pollutants including nutrients, organic compounds, and other emerging chemical contaminants (Gaw et al., 2014; Lytle & Lytle, 2001). The leaching of metabolically active compounds, such as pharmaceuticals, into the environment through runoff or discharge is considered an emerging environmental threat and can have adverse effects on the diversity and structure of ecosystems by creating phytoplankton community shifts, changes in growth and/or reproductive rate, induce behavioural changes or even changes in populations sex ratio (Ford & Herrera, 2019; Hicks et al., 2017; Kaiser et al., 2015; Lopes et al., 2020). Even though it is likely that the amount of each compound being introduced into waterways is generally low (ca. ng/L), their continuous discharge may lead to increasing concentrations and to unknown long-term effects (Küster & Adler, 2014; Petrović et al., 2005). With the advances in medicine and an ever-growing population, the total number of potentially active compounds in circulation has increased (de Oliveira et al., 2016; Gaw et al., 2014). While pharmaceuticals are primarily designed to target humans or bacteria by focusing on well-known metabolic pathways at low doses, this characteristic puts species with a significant number of evolutionary conserved pathways at a higher risk (Duarte et al., 2022a; Gunnarsson et al., 2008), albeit unknown or unpredicted hazardous effects can also occur (Ford & Herrera, 2019). These unintentional effects are not only bound to the animal kingdom, since algae can also suffer a variety of changes in growth rate, increased accumulation of free radicals, changes in their membrane composition and metabolic pathways, and completely block the photosystem II electron transport chain (Duarte et al., 2022a; Nie et al., 2013). Since phytoplankton is one of the main sources of primary energy for most aquatic ecosystems (Lewis, 1995) and is sensitive to pollutants (B. Duarte, Feijão, et al., 2021; Moreira et al., 2006) these organisms, and in specific the diatom *Phaeodactylum tricornutum*,

have been the subject of multiple ecotoxicological studies (B. Duarte, Gameiro, et al., 2021; Renzi et al., 2014; M. M. D. Santos et al., 2002). The sensitivity of the species to both physical and chemical changes (Cabrita et al., 2013, 2014; Moreira et al., 2006; M. M. D. Santos et al., 2002) make it an excellent bioindicator for assessing water quality, and due to its short life cycle, allows for long-term exposure testing in a timely manner. Moreover, this species exhibits a high tolerance for a broad range of environmental factors, including salinity, temperature, and pH, which enhances its value as a bioindicator for environments characterized by significant fluctuations, such as estuaries (Garzke et al., 2019; Geyer & MacCready, 2014; Ringwood & Keppler, 2002).

In recent years the interest in investigating pharmaceutical residues has grown. However, their impact on marine ecosystems has been relatively understudied leaving many gaps in the current understanding of its effects, despite being the final recipient of continental contamination (Branchet et al., 2021). Therefore, it is essential to collect comprehensive pharmaceutical monitoring data to better assess water quality and create adequate regulations. However, *in situ*, testing can present a series of difficulties. Their complexity and cost impose significant limitations on the scope of environmental assessment schemes or scientific studies (Branchet et al., 2021). Although the application of wide monitoring approaches that encompass long-term effects on sensitive species can provide much-needed results representative of real-world environmental conditions, it is imperative that the mechanisms responsible for the field results are understood in controlled conditions before drawing conclusions. Nonetheless, such comprehensive assessments are vital to help corroborate our understanding of the ecological risk these emergent pollutants impose (Branchet et al., 2021).

The immobilization of *P. tricornutum* cells within alginic spheres has been identified as a potentially valuable approach for environmental monitoring, given its cost-effectiveness and efficacy in pollutant detection (Cabrita et al., 2014), however, the capability of these immobilized cells to reveal the effects of pharmaceuticals at environmental concentrations has yet to be evaluated. Although the spheres allow for the passage of nutrients, trace metals, and toxic compounds present in the water column, they also provide the diatom with protection against grazing and the impact of strong water currents. Therefore, preventing their loss into the surrounding medium (Cabrita et al., 2013; Faafeng et al., 1994; Moreira et al., 2006; Moreira-Santos et al., 2004; M. M. D. Santos et al., 2002). Additionally, this method offers a convenient means of transporting, storing, and deploying these algae in the field for ongoing monitoring purposes (Cabrita et al., 2014). As the diatom cells' photochemistry can undergo rapid changes when under stress, optical methods can be employed to detect and quantify these alterations, enabling daily *in situ* measurements, and therefore reducing the overall laboratory workload involved in data collection.

The main objective of this study was to evaluate the effectiveness of immobilized *P. tricornutum* cells as biomonitors for water contamination in environmental samples through the application of non-invasive bio-optical measurements of its main photophysiological parameters and compare it to the anthropogenic pressure that legacy (trace elements) and emerging (pharmaceuticals) contaminants exert by creating a risk matrix based on the measured environmental contaminant concentrations. By detecting fluorescence changes in immobilized *P. tricornutum*, we aim to establish a cost-effective and highly sensitive method for contaminant ecotoxicity assessment in marine field conditions where a myriad of contaminants is present instead of the typical single-compound ecotoxicological exposure. Additionally, the creation of a risk matrix specifically focused on marine algae can serve as a foundation for future projects and contribute to a better understanding of these pressures. Preserving marine ecosystems is of utmost

importance for maintaining biodiversity and promoting human well-being and thus comprehending the impacts of contaminants on these ecosystems represents a significant stride towards their preservation.

2. Materials and Methods

2.1. Study area and sample collection

A total of six water sampling sites were selected, covering four estuaries along the Portuguese coast (Douro, Tejo, Sado, Mira), along with one adjacent coastal site to the Tejo estuary (Cabo Raso) (Figure 1 and Table 1).

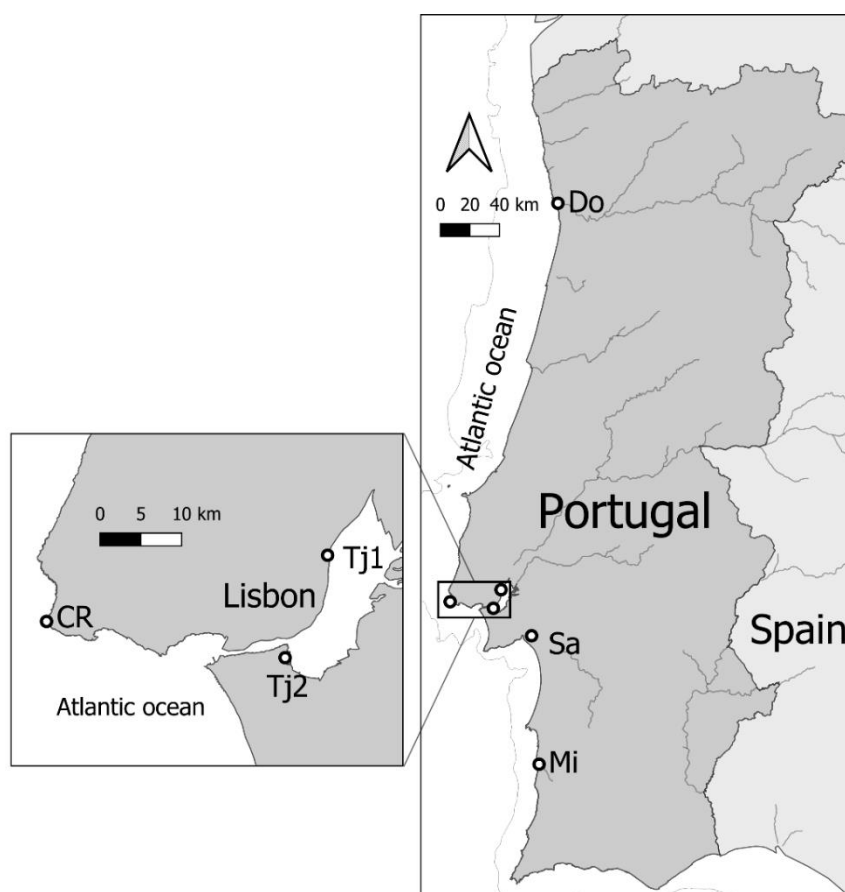


Figure 1. Water collection sites in estuaries along the Portuguese coast, namely in Douro (Do), Tejo (Beirolas-Tj1, Mutela-Tj2 and adjacent nearshore area Cabo Raso-CR) Sado (Sa) and Mira (Mi).

Table 1. Water sampling sites coordinates, mean sample salinity \pm standard deviation and number of samples collected (N).

Site	Type	Coordinates		Salinity (mean \pm SD)	Temperature (mean \pm SD)	N
		Latitude	Longitude			
Do-Douro	Estuary	41.147182	-8.665853	9,4 \pm 0,78	24,83 \pm 0,12	8
CR-Cabo Raso	Coast	38.710016	-9.486147	34,43 \pm 0,05	26,1 \pm 0,14	6
Tj1-Beirolas	Estuary	38.787039	-9.090941	2,14 \pm 0,82	23 \pm 0,05	8
Tj2-Mutela	Estuary	38.673391	-9.149256	14,03 \pm 1,75	17,83 \pm 0,12	6
Sa-Sado	Estuary	38.508316	-8.850270	34,72 \pm 0,46	17,82 \pm 0,12	8
Mi-Mira	Estuary	40.338249	-8.842677	34,53 \pm 4	22,53 \pm 0,09	8

Geomorphological and hydrologic conditions as well as the resident population and wastewater treatment levels in all sampled estuaries are shown in Table 2. The Tejo Estuary spanning an expansive area of 320 km², is situated across the largest metropolitan area in Portugal, supporting a population of 1.84 million people residing in the surrounding municipalities, and representing one of the largest estuaries in Western Europe. However, due to its large size, distinct pollution sources and contaminant variability observed between the urban areas of Lisbon and Almada (Fonseca et al., 2021), sampling two separate distant sites allows for a comprehensive assessment of pollutant levels.

The Douro Estuary is situated within Portugal's second-largest metropolitan region, encompassed by approximately 0.68 million inhabitants. Although both the river area and volume are relatively low, this estuary experiences a higher flow rate compared to others. The second largest estuary in Portugal is Sado (ca. 180 Km²) located south of Tejo estuary, in Setubal district and is characterized by its high volume and smaller population of 257 551 residents. Lastly, the Mira Estuary has the smallest area and the least residential development in its surrounding region. The degree of wastewater treatment that occurs in each estuarine area also varies between sampling areas. The Douro wastewater treatment plants have an even split between secondary and tertiary treatment. On the other hand, the treatment facilities existing at the Tejo Estuary implement all 3 levels of water treatment and more than 50% of the discharges result from secondary-level treatment plants. The Sado and Mira estuaries' treatment plants only provide secondary and tertiary treatment, however, more than 60% are treated at the tertiary level.

The sampling campaign lasted four days from 25 to 29 July 2022. A total of 44 samples were collected, transported in pre-rinsed polyethylene bottles, placed on ice, and kept in the dark. The salinity and water temperature (VWR International, EcoSense® EC300) of each sample were recorded after collection, except for Douro which had its salinity measured in the laboratory.

Table 2. Geomorphologic and Hydrologic characteristics of sampled estuarine systems - Douro, Tejo, Sado, and Mira, along with details on the resident population and wastewater treatment facilities in the surrounding municipalities adapted from (Duarte et al., 2023).

	Unit	WWTP Treatment level	Douro	Tejo	Sado	Mira
Total area ^a	Km ²		10	320	180	5
River Flow ^a	m ³ s ⁻¹		450	300	40	3
Volume ^a	10 ⁶ m ³		4	5	500	27
Resident population ^b	N ^o ^A		683,063	1840523	257,551	24,717
Volume of waste water treated at each level ^b	% ^A	Primary	0	27	0	0
		Secondary	50	57	29	32
		Tertiary	50	16	71	68
Dwellings served by wastewater drainage ^b	% ^B		94	96	88	66

^a (França et al., 2009)

^b Data adapted from Duarte et al., 2023, which utilized 2019 statistics from local municipalities sourced from Statistics Portugal (www.ine.pt). The values presented represent either the summed (A) or averaged (B) data for each estuarine area.

Samples were divided into smaller subsets for the characterization of the trace element and pharmaceutical residue quantification, as well as for testing the exposure effects of the water sample on marine diatoms. Upon lab arrival, each sample was promptly frozen to stabilize any volatile compounds present in the water and kept at -20 °C until analysis or the beginning of the exposure trials.

2.2. Water chemical analysis

After thawing overnight at 10 °C, all samples had their pH adjusted to 3 using formic acid (AnalaR NORMAPUR Formic Acid 99-100%). Trace element concentrations in the water samples were determined using total reflection X-ray fluorescence spectroscopy (TXRF S2 PICOFOX, Bruker, Berlin, Germany). To ensure quality and assurance control (QA/QC) equipment recalibration (gain correction, sensitivity analysis and multi-elemental standards) and analytical blanks were performed. Samples were added with an internal standard (Gallium) (Duarte et al., 2022b) used to determine final elemental concentrations and analysed directly by TXRF. To assess pharmaceutical compounds' concentrations. Subsequently, samples were vacuum filtered through a 1.2- μm glass microfiber filter followed by a 0.45- μm membrane. Samples were purified via solid-phase OASIS HLB cartridges and subsequently washed with 5 ml of 5% methanol 95% water solution and eluted with 6 ml of methanol. The eluent was evaporated under a gentle stream of N_2 at 35°C and the residue was stored in amber vials at -80°C before analysis. Methanolic extracts were hydrated and recovered using a 3:97 methanol-water mixture (500 μL) and were analysed using Ultra High-Performance Liquid Chromatography-tandem mass spectrometry (UHPLC Nexera X2 Shimadzu coupled with a Triple TOF™ 5600+ from AB Sciex). The UHPLC system included a vacuum degasser, an autosampler (with an injection volume of 10 μL and set at 10 °C), and a binary pump with a reverse-phase analytical column (Zorbax Eclipse Plus C18–2.1 \times 50 mm, 1.8 μm , Agilent) set to 40 °C. The experimental protocols were adapted from the literature sources Chau et al., (2017), Fonseca et al., (2021), Freitas et al., (2014), Santos et al., (2016). Samples were screened for 69 different drugs (Supplement Table 1). Compound concentration was determined using MultiQuant™ software. A calibration curve was constructed using the chromatographic peak areas, with a concentration range of 0.8 ng/L to 10 ng/L. Calibration curve linearity was assessed in each batch of samples and deemed acceptable if the correlation coefficient was above 0.99. During validation, detection, and quantification limits (LOD and LOQ) were calculated using signal-to-noise ratios (S/N) of 3 and 10, respectively. The concentrations of the pharmaceutical compound in the water are expressed as micrograms (μg) per liter.

2.3. Experimental Procedure

Phaeodactylum tricornutum Bohlin (Bacillariophyceae; strain IO 108-01, IPMA) axenic and monoclonal cell cultures were grown in 250 ml of f/2 medium (Guillard & Ryther, 1962), under constant aeration at 18 ± 1 °C. Cultures were grown for 4 days in a growth chamber (Fytoscope FS130) with a sinusoidal light function, with a light intensity at noon of RGB 1:1:1 and a maximum PAR of 80 $\mu\text{mol photons m}^{-2} \text{ s}^{-1}$, and operated under a 14/10 h day/night cycle. These growth chamber conditions have been previously described by Feijão et al., (2018).

For the alginate bead production, an alginate solution was prepared with a 2% (w/v) alginic acid sodium salt extracted from brown algae (Sigma-Aldrich) and adjusted to 35 ppm before gently mixing with *P. tricornutum* (5 500 000 cells/ml) stock culture. Alginate beads polymerization was performed by dropping aliquots of the alginic-*P. tricornutum* gel (55 280 000 cells/ml), in a solution of 5% (w/v) CaCl_2 for 5 minutes. Both solutions (5% CaCl_2 and 2% alginic solution) had their salinity adjusted to 35 ppt with NaCl. The hardened beads were placed in pairs

within 24-well plates. Each well was filled with filtered (0.45- μm membrane) and salinity-

Table 4. Chlorophyll fast induction kinetics derived parameters adapted from Duarte et al., (2021). adjusted (35 ppm) water samples from the different environmental sites prior to exposure. Each plate housed three replicates per sample and an additional 4th replicate that was added with 100 $\mu\text{L/L}$ Glyphosate to act as a negative control due to its high toxicity (Cruz de Carvalho et al., 2020). These glyphosate-exposed beads allow to confirm the entry of large organic molecules and in case of toxicity (such as the one imposed by the tested glyphosate degree) the cells reflect these negative effects. Exposure lasted for 7 days in a growth chamber (according to the conditions abovementioned) with photobiological assessments performed daily at a consistent time. To assess the photobiological performance of the immobilized cells, the OJIP test was used using a Chlorophyll *a* Pulse Amplitude Modulated (PAM) Fluorometer (Photon Systems Instruments (PSI), FluorPen FP 100) (B. Duarte, Feijão, et al., 2021). The test is made out of four distinct phases: the first phase is level O representing all open reaction centers with no reduction of Q_A which lasts for 10 ms; the second phase is the transient curve from O to J indicating the net photochemical reduction of QA lasting for 2 ms; the third main phase J to I represents the reduction of all the reduced states of closed RCs such as $Q_A^-Q_B^-$, $Q_AQ_{B2}^-$, and Q_A-QBH_2 , which lasts for 2-30 ms; the final phase P represents the rate of utilization of the chemical (potential) energy and the rate of dissipation (B. Duarte et al., 2019; B. Duarte, Gameiro, et al., 2021; Zhu et al., 2005). Each step (O-J, J-I, and I-P) of the Kautsky curve is associated with different physical-chemical events in the PSII, and by analysing each section it is possible to determine the performance of multiple photo-physiological parameters (Table 3).

Table 3. Chlorophyll fast induction kinetics derived parameters adapted from Duarte et al., (2021).

F_o	Basal fluorescence (at $t=0$)
PI	Performance Index
ABS/RC	Absorbed energy flux per reaction center
TR_o/RC	Trapped energy flux per reaction center
Relative TR, TR (%)	Relative Trapped energy flux normalized towards the absorbed energy flux $(TR_o/RC)/(ABS/RC) \times 100$
ET_o/RC	Transported energy flux per reaction center
Relative ET, ET(%)	Relative Transported energy flux normalized towards the trapped energy flux $(ET_o/RC)/(TR_o/RC) \times 100$
DI_o/RC	Dissipated energy flux per reaction center
Relative DI, DI (%)	Relative Dissipated energy flux normalized towards the absorbed energy flux $(DI_o/RC)/(ABS/RC) \times 100$
SFI	Structural and Functional Index of the Photochemical Reactions
SFI (NPQ)	Structural and Functional Index of the Non-Photochemical Reactions

2.4. Data analysis

The Pollution Load Index (PLI) (Eq. 1) was used as a mathematical model to summarize environmental concentrations of As, Cr, Cu, Mg, Pb, Ti, and Zn into a single value. C_f represents the concentration of the i^{th} metal and n is the number of analysed metals.

$$PLI = \left[\prod_{i=1}^n CF_i \right]^{1/n} \quad (1)$$

Since the PLI is calculated as the geometric means of concentrations it is less influenced by extremely high or low concentration values and can provide a useful pollution range that is comparable between estuaries (Tomlinson et al., 1980). 4 classes can be distinguished for

pollution metal characterization: $PLI < 1$ corresponds to unpolluted samples, $1 < PLI < 2$ moderately polluted, $2 < PLI < 10$ strongly polluted, and $PLI > 10$ extremely polluted samples (Radomirović et al., 2020). This classification allows a simplification of results and in turn provides valuable insight to the policymakers and the general public, classifying the samples by their complete metal profile in opposition to the classic evaluation of each of the elements present in the sample (Tomlinson et al., 1980).

The potential chemical hazard of water samples was also analysed via risk assessment analyses, using the Measured Environmental Concentrations (MEC) and the Predicted No Effect Concentrations (PNECs). Bibliographical data regarding the ecotoxicity of the measured pharmaceuticals and trace-metals was compiled for the test species, whenever available. Selected data followed the preference *P. tricornutum* > Marine diatoms > Green algae however when none was available ECOSAR was used to estimate Toxicological Data (ECOSAR, 2012). Due to the limited availability of data regarding chronic endpoints in estuarine conditions, acute freshwater endpoints were predominantly used. This approach is considered the best practice in the absence of data regarding specific test conditions (ECHA, 2003; Riva et al., 2019). By using more readily available acute endpoints we were able to create a more comprehensive understanding of the potential risks. Because of this, only short-term/acute endpoints were used for PNEC. PNEC was estimated by dividing the lowest toxicity value by their respective Assessment Factor (AF) which is 1 000 for freshwater species or 10 000 for marine/brackish species (Riva et al., 2019). The separation allows for the extrapolation of laboratory data from single-species to multi-taxa ecosystems while taking into account uncertainties related to biological and experimental variability (Fonseca et al., 2021). Risk Quotients (RQ) were obtained by dividing the highest Measured Environmental Concentration (MEC) by the PNEC respective to each organism and pharmaceutical. Additionally, it was considered that if the RQ is equal or exceeds 1 then it presents a high ecological risk requiring regulatory actions (ECHA, 2008). Following the thresholds presented by Minguez et al., (2016). we also considered the classifications: no risk ($RQ < 0.01$), low risk ($0.01 \leq RQ < 0.1$) and moderate risk ($RQ \geq 0.1$) (ECHA, 2008; Hernando et al., 2006).

The toxicity assessment regarding pharmaceuticals in a mixture was based on the methodology proposed by Backhaus and Faust, (2012). The authors propose two ways of calculating risk: $RQ_{PEC}/PNEC$ and RQ_{STU} . However, both equations require the use of toxic information regarding multiple taxa and since the risk matrix was performed only with algae, a simplified version of $RQ_{PEC}/PNEC$ was used where the RQ for crustaceans and fish was assumed 0. $RQ_{PEC}/PNEC$ is the sum of the Risk Quotients (RQ) for each pharmaceutical considering the lowest concentration capable of eliciting metabolic response. Additionally, the Assessment Factor (AF) can be 1,000 or 10,000 depending on the environment. The equation can also be modified to integrate Measured Environmental Concentrations (MEC) instead of predicted environmental concentrations (e.g., Riva et al., 2019 (Eq. 2)). However, summing all RQs regarding different organisms has its inherent limitations in accuracy, and $RQ_{PEC}/PNEC$ equation is recommended to conservatively measure RQ and it is recommended as a first-tier approach (SCHER, SCCS, SCENIHR, 2012). As per the European guidelines (ECHA, 2003), it is recommended to combine information for freshwater and brackish/marine species. The assessment should be based on the most sensitive organism for each therapeutic class.

$$RQ_{\frac{MEC}{PNEC}} = \sum_{i=1}^n \frac{MEC_i}{PNEC_i}$$

$$RQ_{\frac{MEC}{PNEC}} = \sum_{i=1}^n \frac{MEC_i}{\min(EC50) \times (\frac{1}{AF_i})} \quad (2)$$

A Principal Component Analysis (PCA) of pharmaceuticals and metal concentrations found at each site was used to assess spatial contamination patterns and to visualise possible hidden relations between contaminants. Canonical Analysis of Principle (CAP) coordinates, using Euclidean distances, was performed using the photo biological data obtained over the exposure and used to search for dissimilarities in physiological parameters and to indicate the time point with the highest overall classification to base other tests. CAP and data normalization for the PCA was performed using PRIMER 6 version 6.1.13 & PERMANOVA+ version 1.0.3 from PRIMER-e. Non-parametric, Kruskal-Wallis pairwise tests were performed to determine significant differences among sites and variables. To determine possible physiological responses regarding specific environmental concentrations a Spearman's correlation analysis was utilized. PCA, Kruskal-Wallis pairwise tests, and Spearman's correlations were performed using R version 4.2.2 (R Core Team, 2022) and results were considered significant when $p < 0.05$.

3. Results

3.1 Water chemical characterization and risk assessment

Pharmaceuticals were found in all samples, with 23 different compounds detected out of the 69 screened (Table 4, and Supplement Table 2). Overall, a minimum of 2 (CR) and a maximum of 23 (Tj1) pharmaceuticals per sample were detected. Only two therapeutic groups had a detection frequency above 95%: β -blockers (Bisoprolol and Propranolol had 100% detection frequency) and antibiotics. Antibiotics were the therapeutic group with the highest number of pharmaceuticals found, however β -blockers, antihypertensive and antidepressants were the classes with the highest recorded concentrations across all samples (Figure 2B, 2C and 2D). The samples collected at Tj1 and Tj2 consistently presented median pharmaceutical concentrations above the ones assessed in the other sampling sites (Figure 2A).

Samples from the Tejo estuary with the lowest mass load (Tj2 at 756.74 ng/L) were vastly larger than the sample with the highest concentration from outside the estuary (CR at 36.74 ng/L). Cabo-Raso had the sample with the highest pharmaceutical mass load outside of Tejo, followed by Douro estuary samples with the third highest median concentration of 30.22 ng/L (Tj1 and Tj2 being the highest, 1898.88 ng/L, and second highest, 1198.2 ng/L, respectively). The samples collected in Sado and Cabo-Raso have similar median values of 22.92 ng/L and 21.36 ng/L respectively, while Mira samples had the lowest median value of 13,82 ng/L.

Antidepressants had the highest cumulative compound mass among all other classes, totaling 7303.97ng and a maximal load of 1283.07 ng/L in a single Tj1 sample (Figure 2B). However, this is due to a spike in Venlafaxine concentration detected in samples from both sites in the Tejo estuary. Excluding Venlafaxine, the total drops to 810.38 ng/L, and a new maximum concentration per sample is obtained at 140.08 ng/L also at Tj1.

β -blockers also demonstrated high cumulative values at 1944,80 while lipid regulators antibiotics, anxiolytics, and analgesics represent the groups with the lowest total detected mass across all samples (Figure 2C, 2G, 2H, 2I, and 2J). Antibiotics were the therapeutic group with the greatest variety of compounds detected, but they were mostly at relatively low concentrations. Among the nine therapeutic groups detected, Tj1 had the highest median concentrations per site for five groups, while the remaining four groups (NSAID, β -blockers, lipid regulators, and analgesics) showed their maximum median concentrations per site at Tj2. However, the samples collected from Douro another very urbanized estuary, were mainly composed of antidepressants, antihypertensives, and anticonvulsants.

Both Mira and Sado samples were mainly influenced by β -blockers, antidepressants and antihypertensives (Figure 2B, 2C, 2D). Now, pharmaceutical concentrations in the water can vary greatly depending on season and time of day, and singular water grab events do not account for such variation (Duarte et al., 2023). Therefore, all the concentrations detected are merely a

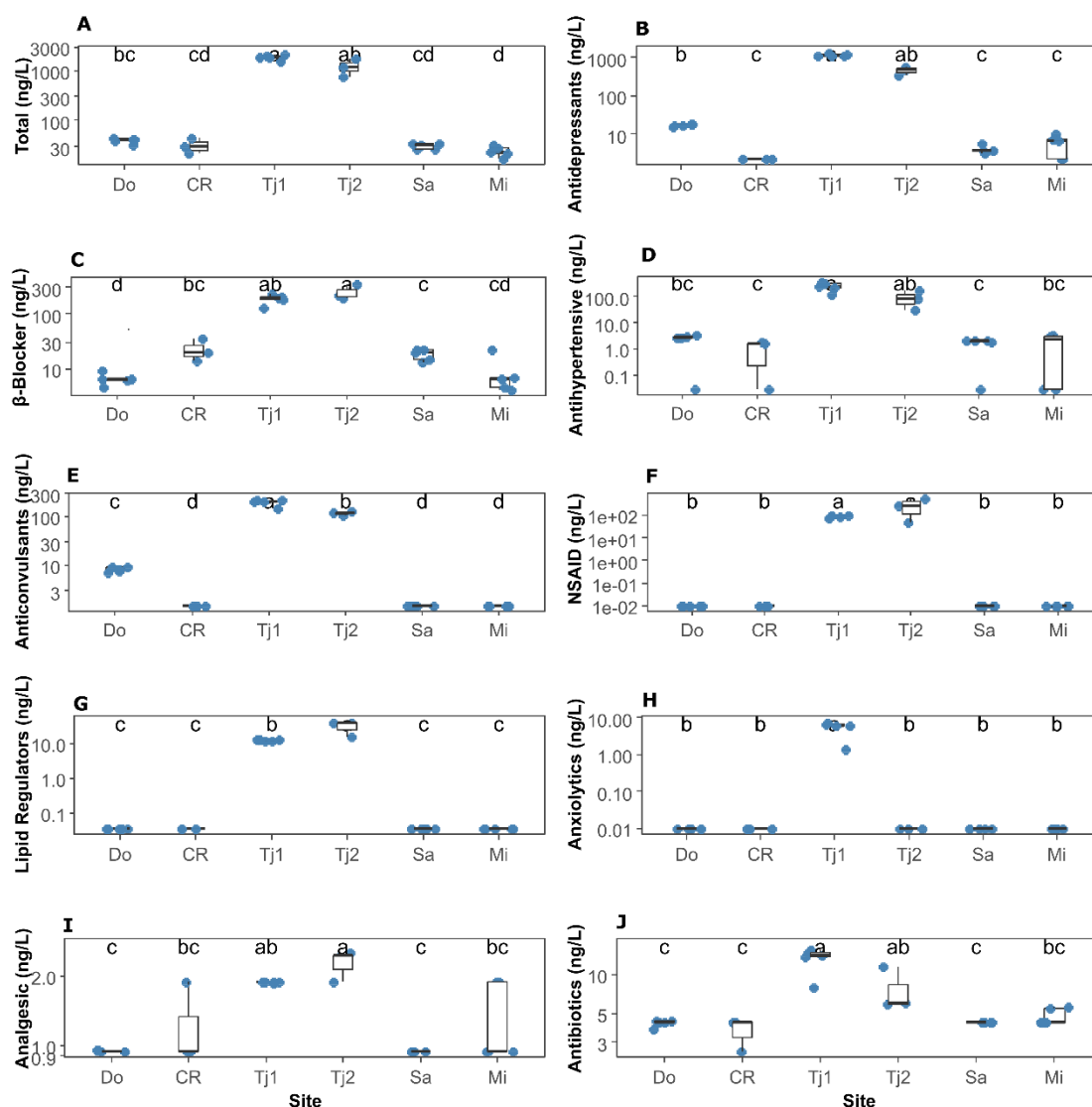


Figure 2. Pharmaceutical concentration in water samples by therapeutic group (ng/L) across all sampling sites (Do-Douro Estuary N=5 ; CR – Cabo Raso N=3 ; Tj1 and Tj2 – Tejo Estuary Sampling Site 1 and 2, N=5 and N=3 respectively; Sa – Sado Estuary N=5; Mi – Mira Estuary N=5) (letters denote significant differences at $p < 0.05$) by therapeutic group.

snapshot of water conditions at that specific time and may yield different pharmaceutical concentrations and proportions depending on the time of collection. Within each therapeutic group, the concentrations of each compound varied.

Anticonvulsants had the highest median value of all therapeutic groups at 115,26 ng/L and a max concentration per sample of 215,11 ng/L in Tj1 (Figure 2E). However, since only Carbamazepine was detected above LOQ, it's the only contributor to the sample median values in the only three sites that detected it. The median values of Carbamazepine in samples from each site varied vastly Tj1 with 202.69 ng/L, Tj2 with 114,98 ng/L, and Douro with 4.97ng. Tj1, Tj2 and Douro show a 100% detection rate for Carbamazepine and Lorazepam.

NSAID demonstrated the second-highest median value of 88 ng/L. Diclofenac was the only NSAID detected in any samples. With a 100% sample detection rate in Tj1 and Tj2. The median and maximal Diclofenac sample concentration was considerably lower in Tj1 samples (84 ng/L median 511.21 ng/L maximal) compared to Tj2 samples (276.21 ng/L median 95.74 ng/L maximal) (Figure 2F).

The β -blockers, specifically Bisoprolol and Propranolol had a detection frequency of 100% across all sites, making them the only therapeutic group with a 100% detection rate (Figure 2D). Atenolol showed a lower detection frequency of 23% across all samples but it was more prevalent in Tj1 (80% detection) and Tj2 (66.67% detection) samples. Bisoprolol reached its highest median concentration in Tj1 water samples (116.43 ng/L) and in Tj2 samples (92.93 ng/L). Both Sado and Cabo-Raso samples had similar medians for Bisoprolol (18.56 ng/L and 18.23 ng/L respectively), while Douro samples showed the lowest median value of 1.48 ng/L. Despite the frequent detection of Propranolol, the median concentration ranged from 1.26 ng/L in Sado samples to 4.3ng in Tj1. Atenolol on the other hand ranged from 42.9 ng/L in Tj1 to 44.02 ng/L in Tj2.

As previously mentioned, antidepressants concentrations varied greatly between compounds and samples. Venlafaxine had the highest detection rate in antidepressants at 88,77% across all samples. Notably, the max Venlafaxine concentration in a singular sample reached 1143.41 ng/L in Tj1 (Figure 2B). Venlafaxine also reached a median value of 1028.98 ng/L in Tj1 and 379.91 ng/L in Tj2 samples. In contrast, the Douro samples, whose only detected antidepressant was Venlafaxine had the third highest concentration and only reached a median value of 15 ng/L. Samples from Mira and Sado also detected Venlafaxine at lower concentrations between 1.11 ng/L and 8.54 ng/L. Sertraline and Venlafaxine were the only antidepressants detected in both Mira and Sado water samples while samples collected at Cabo-Raso had no detection of antidepressants. The maximum median concentration of Sertraline was similar to Escitalopram (21.60 in Tj2 ng/L for Sertraline and 29.73 ng/L for Escitalopram in Tj1). Escitalopram and Citalopram were only detected in water samples coming from the Tejo estuary and Citalopram concentrations were always above Escitalopram.

The class of lipid-regulators, anxiolytics, and analgesics each consisted of a single compound and were almost entirely detected in Tejo water samples (Figure 2G, 2H and 2I), except for the analgesic Acetaminophen, which was detected below LOQ in Mira and samples. The class lipid-regulators is composed entirely of bezafibrate whose median values are higher in samples collected in Tj2 (37.65 ng/L) than in samples from Tj1 (12.63 ng/L). The anxiolytic Alpha-Hydroxyalprazolam was only detected in Tj1 samples at concentrations between 7.16 ng/L and 1.42 ng/L (Figure 2H) while the analgesic Acetaminophen was only detected above LOQ in water samples from Tj2 at concentrations between 1.88 ng/L and 2.5 ng/L (Figure 2I).

The antihypertensive class was detected in varying concentrations at all sites (Figure 2D). Water samples from Tj1 and Tj2 both exhibited a 100% detection rate of Indapamide, Irbesartan and Losartan. The median values of Indapamide between Tj1 and Tj2 samples are not drastically different being only 1.1 ng apart. However, Irbesartan has a median value of 245.05 ng/L in the Tj1 water samples, while only reaching 71.14 ng/L in Tj2 samples. Conversely, Losartan has a higher median concentration of 125.62 ng/L in water samples from Tj2 than in Tj1 only reaching 36.16 ng/L. Irbesartan had the most dispersion across sites, being detected in water samples of all sites. Yet, the median Irbesartan concentration in Tj1 samples of 245.05 ng/L is by far the highest median antihypertensive value.

Antibiotics demonstrated an overall detection frequency of 96.15% (Figure 2J). However, Ciprofloxacin, the most frequently detected antibiotic, was only found at concentrations below LOQ. Sulfamethoxazole, Sulfapyridine and Trimethoprim were also detected at concentrations below LOQ in Tj1 water samples and Sulfapyridine was also detected below LOQ in Tj2 samples. Azithromycin was detected in samples from Tj1, Tj2, Douro, and Mira samples and had the highest median value among antibiotics of 6.2 ng/L and 6.41 ng/L at Tj1 and Tj2 respectively. Doxycycline had the second-highest median values of 2.97 ng/L and 1.49 ng/L at Tj1 and Tj2 samples respectively. Flumequine was only detected above LOQ in Tj1 samples.

Table 5. Summary of the 23 pharmaceuticals from 7 therapeutic groups detected (N= 26 water samples). Includes detection frequency (%), median, minimum, average (Standard Error), and maximum concentrations (ng/L⁻¹). (< LOQ = below limits of quantification).

Therapeutic Group	Pharmaceutical	Detection Frequency (%)	Median (ng/L)	min (ng L ⁻¹)	mean (se) (ng L ⁻¹)	max (ng L ⁻¹)
Analgesic	Acetaminophen	42,31	0	<LOQ	<LOQ	<LOQ
Anxiolytic	AlphaHydroxyalprazolam	19,23	0	1,42	1,06 (0,46)	7,16
NSAID	Diclofenac	30,77	0	47,8	48,67 (3,55)	511,22
Lipid-Regulator	Bezafibrate	30,77	0	11,6	5,92 (0,51)	39,14
Anticonvulsant	Carbamazepine	50	2,14	4,28	51,26 (2,12)	214,53
	Lorazepam	50	<LOQ	<LOQ	<LOQ	<LOQ
	All	50	2,15	4,3	51,39 (15,46)	215,12
β-blocker	Atenolol	23,08	0	31,2	9,78 (15,42)	49,15
	Bisoprolol	100	18,4	0,64	41,24 (0,03)	132,71
	Propranolol	100	1,33	0,66	1,92 (7,29)	5,2
	Losartan	46,15	0	3,13	21,86 (79,94)	202,99
	All	100	19,7	4,11	52,94 (12,43)	187,06
Antibiotic	Azithromycin	34,62	0	1,13	1,52 (21,61)	7,48
	Ciprofloxacin	88,46	<LOQ	<LOQ	<LOQ	<LOQ
	Doxycycline	42,31	0	<LOQ	<LOQ	3,18
	Flumequine	19,23	0	0,09	<LOQ	0,12
	Sulfamethoxazole	15,38	0	<LOQ	<LOQ	<LOQ
	Sulfapyridin	26,92	0	<LOQ	<LOQ	<LOQ
	Trimethoprim	19,23	0	<LOQ	<LOQ	<LOQ
	All	96,15	0,37	0,08	2,47 (0,71)	11,09
Antidepressant	Citalopram	26,92	0	52,7	21,82 (8,97)	104,75
	Escitalopram	26,92	0	17,6	<LOQ	34,92
	Venlafaxine	80,77	10,76	1,11	249,75 (1,16)	1143,41
	Sertraline	23,08	0	1,95	2,08 (0)	26,47
	All	80,77	10,76	1,11	280,92 (89,3)	1283,07
Antihypertensive	Indapamide	30,77	0	2,68	1,66 (0)	6,72
	Irbesartan	80,77	2,66	1,56	57,25 (0)	329,63
	All	80,77	2,66	1,56	80,78 (25,57)	375,52

The detected trace metal concentrations were relatively low across all samples and most elements revealed no significant differences (Figure 3). All metals had a 100% detection rate apart from Arsenic (Figure 3A) which was only detected in Sado and Mira samples, and Titanium, which was not detected in any Sado sample (Figure 3B). Overall, the combined trace metal weight

per water sample had its highest median of 0.78 mg/L in Mira samples, followed by samples from Cabo-Raso and Tj2 both with 0.4 mg/L. The combined trace metal weight per water samples from Douro and Tj1 had the lowest values of 0.37 mg/L and 0.3 mg/L respectively.

The overall metal concentrations within each site varied. Samples from Mira had the highest median concentrations for Arsenic (0.09 mg/L), Lead (0.52 mg/L), and Titanium (0.12 mg/L) (Figure 3A, 3B, and 3C). The elements Chromium and Copper had their maximum median concentrations in Sado samples (0.28 mg/L and 0.02 mg/L respectively) (Figure 3D, and 3E), while Zinc had its maximum median concentration of 0.156 mg/L in Tj2 samples (Figure 3F). CR, Tj1, and Tj2 samples had a higher Zinc content than other samples (Figure 3F). Lead was the element with the highest median in Douro samples with 0.12 mg/L followed by Chromium

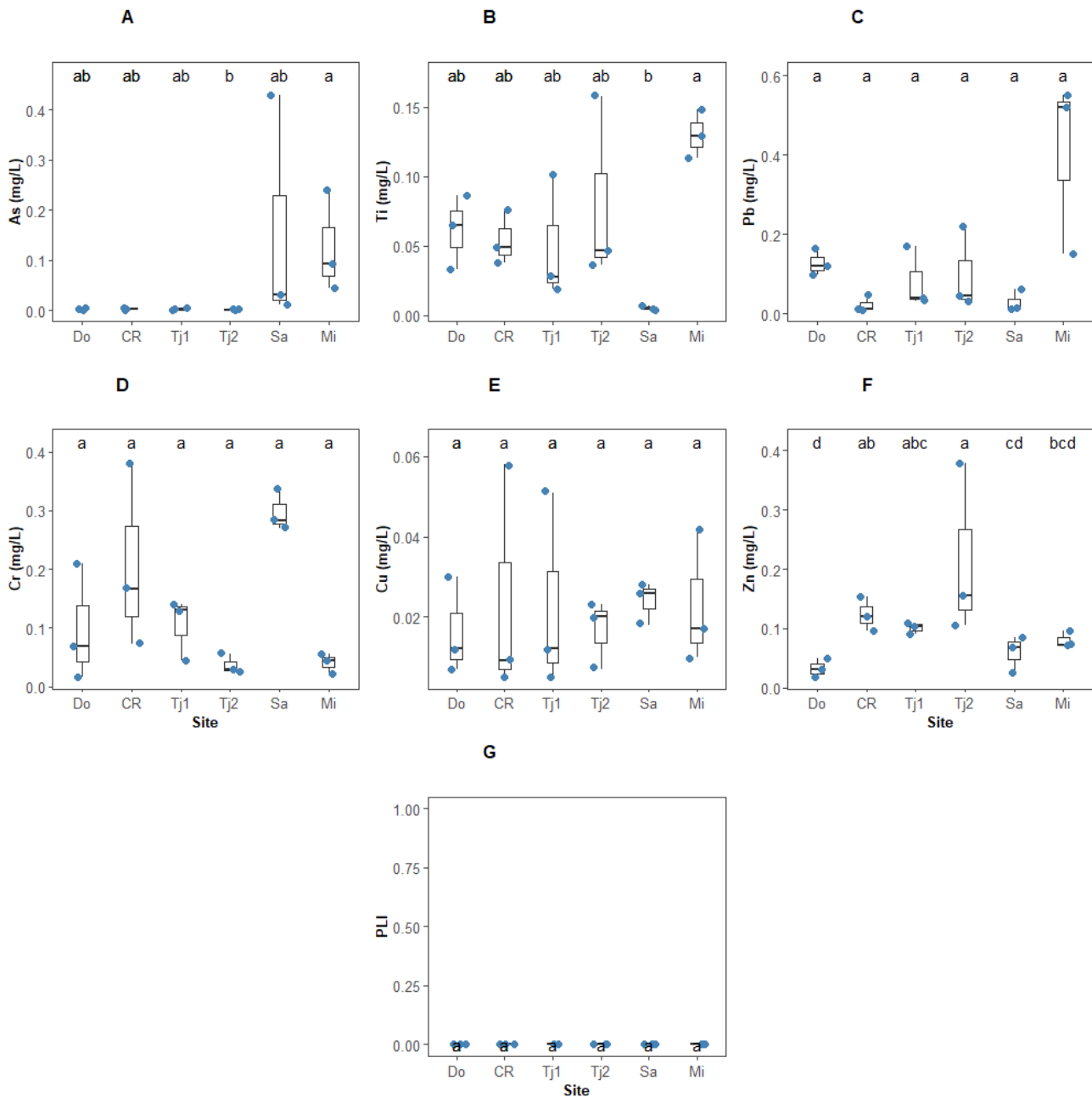


Figure 3. Trace metal concentrations (mg/L) across all sampling sites (Do-Douro Estuary; CR – Cabo Raso; Tj1 and Tj2 – Tejo Estuary Sampling Site 1 and 2 respectively; Sa – Sado Estuary; Mi – Mira Estuary) (N=3 per site, letters denote significant differences at $p < 0.05$)

and Titanium (Figure 3B, and 3D) with similar medians of 0.06 mg/L. Samples collected in Cabo-Raso have a higher medium chromium content of 0.16 mg than other metals in the same sample (Figure 3D), followed by their median zinc content with concentrations of 0.12 mg (Figure 3F). Due to low trace metal concentrations in the water, the PLI was calculated to be 0 for all samples.

A clear separation of the samples can be observed with a PCA. The first two PCA components were able to explain 62.6% of the variance in environmental (metal and pharmaceutical) data (Figure 4). PC1, which has a strong positive influence with pharmaceuticals are capable of explaining 46.96% of all variance in the environment, while PC2 is mainly associated with elements. The PCA also clearly separates both Tejo sites from all other sites due to their pharmaceutical content.

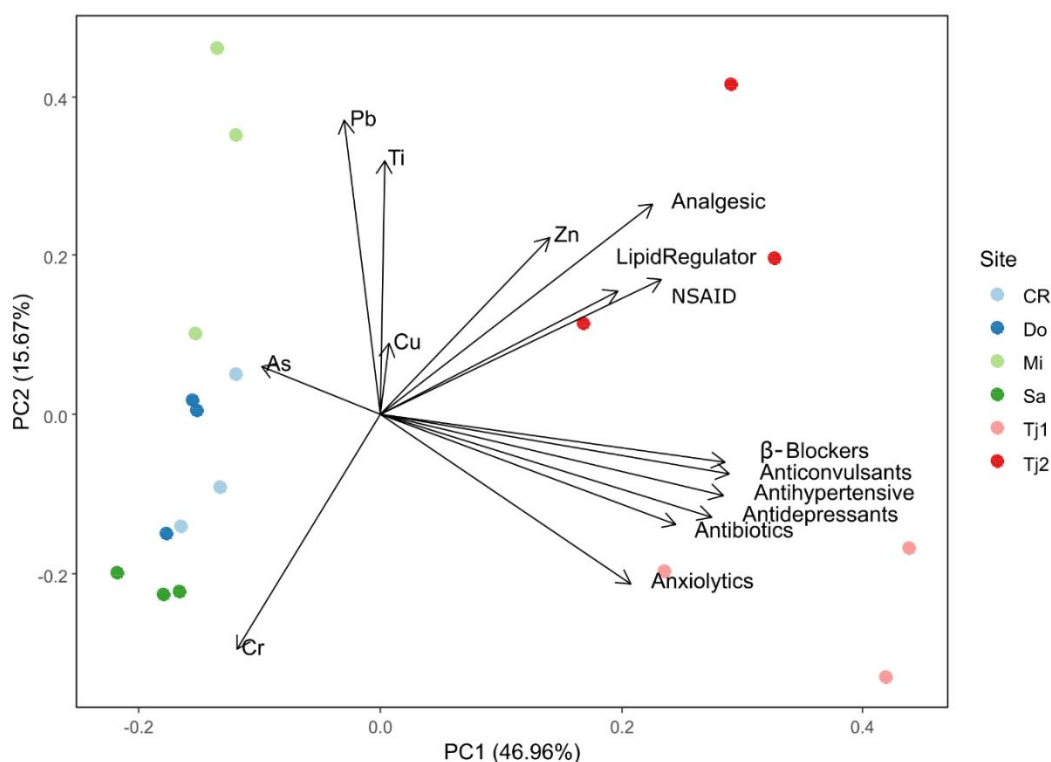


Figure 4. Principal component analysis (PCA) of Pharmaceuticals and metal concentrations found at each site. (Do – Douro, CR – Cabo Raso, Tj1 – Tejo 1 Beirolas, Tj2 – Tejo 2 Mutela and Mi – Mira)

By analysing the maximum measured environmental concentrations and calculating Risk Quotients (RQs), the potential ecological risks associated with pharmaceutical compounds is simplified into several categories facilitating informed decisions for environmental conservation and management. Based on the maximum Measured Environmental Concentration (MEC) obtained. Five compounds were categorized as moderate risk for having RQ between 0.1 and 1 (Figure 5A). These moderate-risk environmental stressors are Losartan, Ibersartan, Ciprofloxacin, Venlafaxine and Citalopram. The highest RQ (0,83) was Losartan which was calculated based on the EC50 of the marine diatom *Cyclotella meneghiniana* (Fonseca et al., 2021). Only two pharmaceuticals had their endpoints estimated through ECOSAR, and both compounds, namely, Doxycycline and ibersartan are classified either as moderate or no risk compounds (Figure 5A). Out of the twenty-three pharmaceuticals detected, seven were classified as low risk environmental stressors and eleven had RQ's below the 0.01 threshold indicating no environmental risk (Figure 5A).

β -blockers (0,85 RQ), Antidepressants (0,63 RQ), Antihypertensives (0,48 RQ) and Antibiotics (0,37 RQ) were the only therapeutic groups in the moderate-risk category. Antidepressants with an RQ of 0.88 (Figure 5B), were influenced by the presumed atypical spike in Venlafaxine. Nonetheless, despite how atypical it may be, such spikes may happen again and should be considered. NSAID, lipid-regulators, anxiolytics and analgesics are composed of a single pharmaceutical and have the RQ of their corresponding compound (Figure 5B).

Overall, all sites represent a moderate to high ecological risk. Samples collected at Tj1 and Tj2 surpassed the critical threshold of one (RQ of 1.53 and 2.12 respectively), indicating high potential environmental risk (Figure 5C). Tj1 is the only site affected by all the therapeutic groups detected, and its main stressors are antidepressants which contribute to over 41% of Tj1 total RQ. Tj2's main stressors are β -blockers with site-specific RQ of 0.85, followed by antidepressants and antihypertensives, both with a site-specific RQ above the Moderate risk threshold. In the water samples of the remaining sites, antibiotics were the highest contributor, being the only pharmaceutical class to consistently obtain a site-specific RQ above 0.1. The water samples collected in Mira and Sado are also the only samples where β -blockers reached a no-risk site specific threshold.

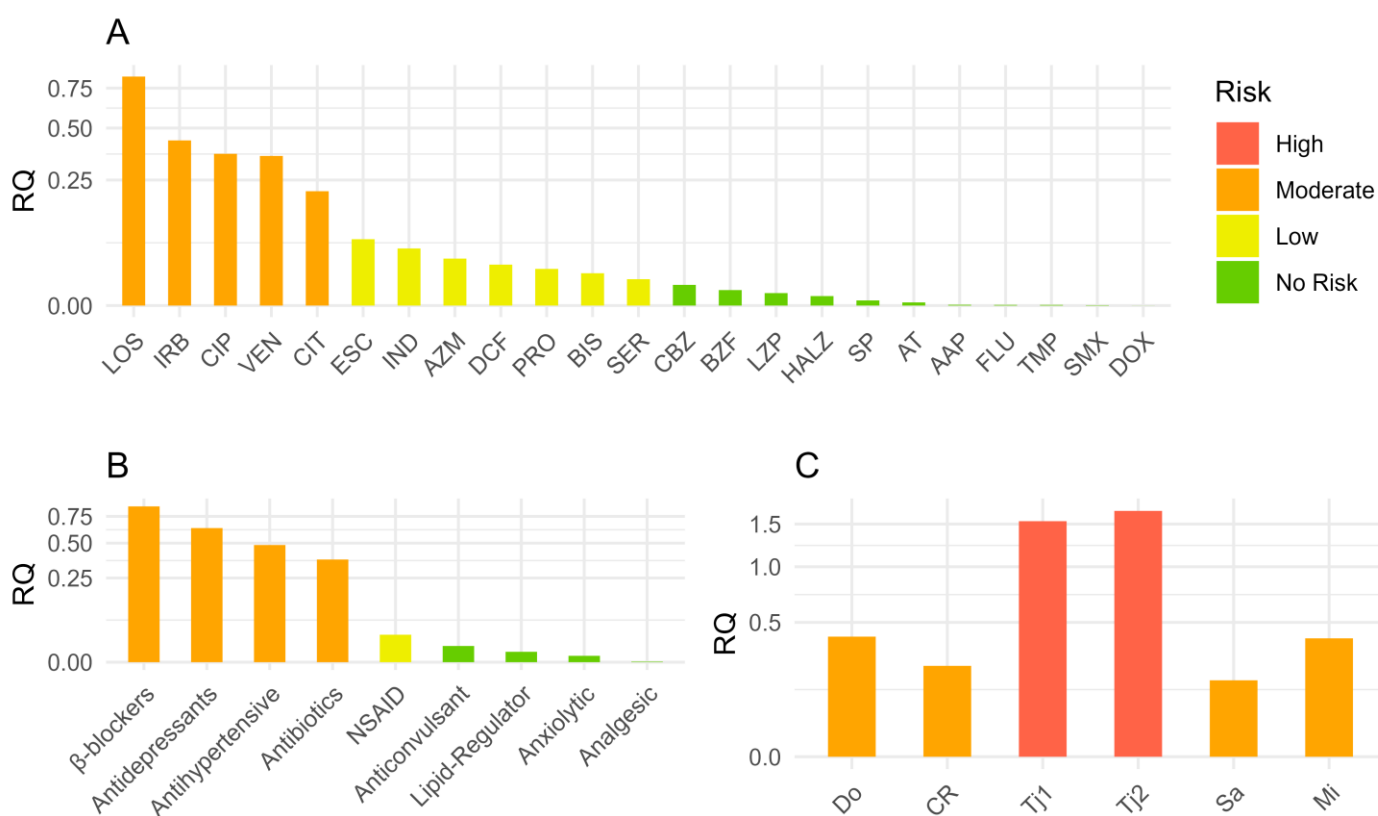


Figure 5. Risk quotients (RQ) of the maximum concentration detected for each pharmaceutical (A), therapeutic Group (B), and each sampled site (C).

3.2 Immobilized diatom exposure trials

The Kautsky curves obtained from the immobilized diatoms indicate a gradual decrease in the fluorescence of the OJIP phases, evident through the inflection points along the curve, during the exposure. The J step, for most sites, showed a gradual reduction in its maximum fluorescence, which becomes more pronounced after the 48-hour mark. Subsequently, both the I and Peak phases start to substantially deteriorate past the 72h mark. This loss of inflection points is consistent with damage at the photosynthetic level or loss of photosynthetic efficiency across all sites during exposure (Figure 6). From the 48h time point forward, diatoms exposed to water from Douro estuary (Do), Cabo Raso (CR) and Tejo estuary sites (Tj1 and Tj2) exhibit progressively diminishing maximum fluorescence than diatoms exposed to water samples from the Sado (Sa) and Mira (Mi) estuaries (Figure 6). Although loss of inflection of the typical OJIP fluorescence profile is visible starting at 48h, past the 96h time point all diatoms display dramatic losses of inflection. While samples from Tj1 displayed the highest pharmaceutical mass load and Tj2 samples registered the highest RQ, diatoms from both sites showed a slower gradual decrease in peak fluorescence than diatoms exposed to Douro water samples. Interestingly, despite Sado samples revealing the lowest RQ it was the diatoms in Mira samples that suffered the least reduction in peak fluorescence in 144 hours. These shifts in the inflection points show that diatoms exhibited a vastly different response depending on the environmental stressor present.

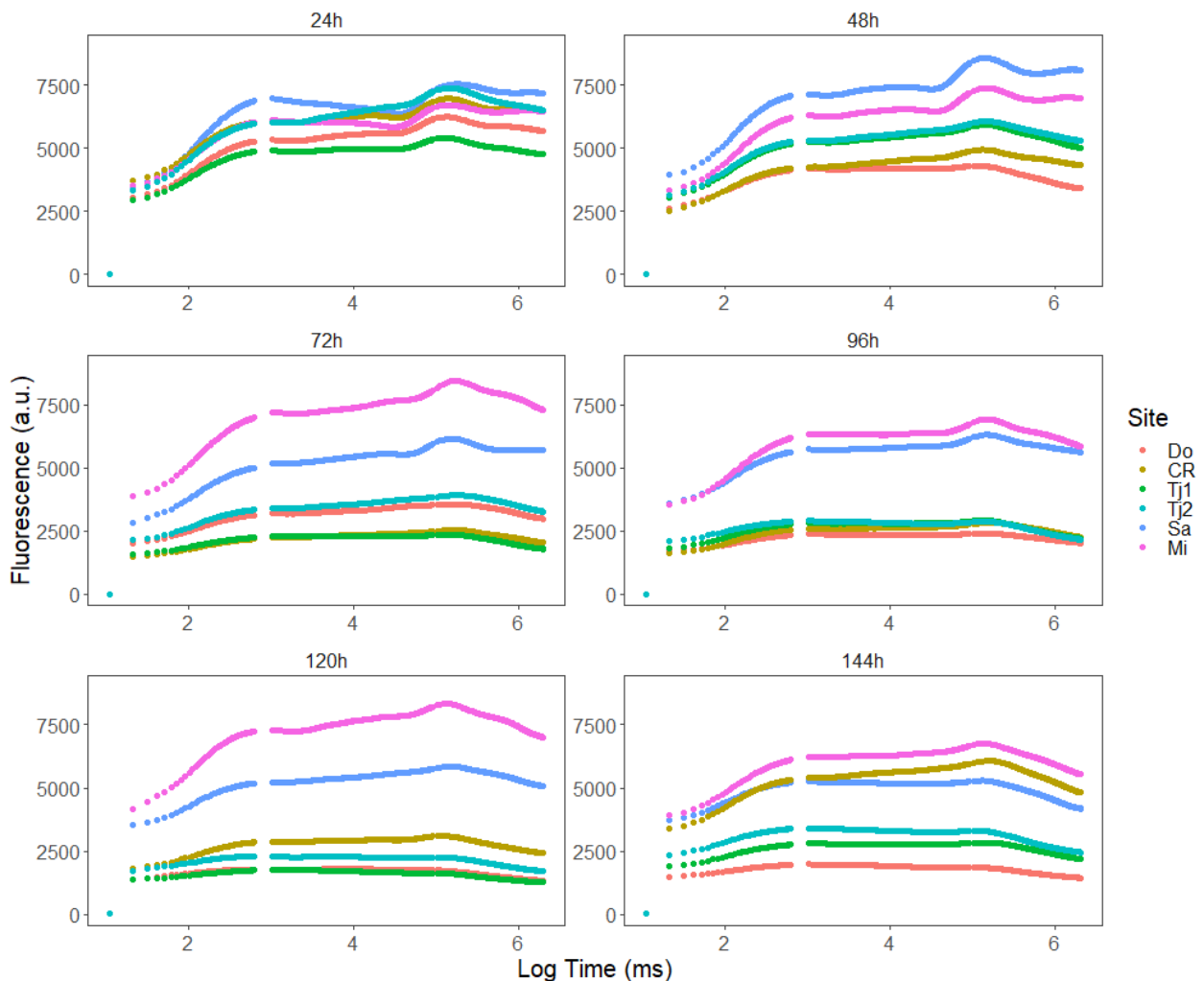


Figure 6. Variable fluorescence curves, following chlorophyll a fluorescence induction curves of *Phaeodactylum tricornerutum* cultures from all sampled sites over 6-day period (Do – Douro, CR – Cabo Raso, Tj1 – Tejo 1 Beirolas, Tj2 – Tejo 2 Mutela and Mi – Mira) (average, N=3 per site)

Using a multivariate CAP analysis, it was possible to evaluate at which time point the fluorescence datapoints were more efficient in separating the diatom samples according to the water samples to which they had been exposed. This was evaluated throughout the model overall efficiency in classifying the samples according to their photochemical traits, with higher model efficiencies corresponding to more contrasting photochemical features between groups allowing better discrimination of samples between water exposure groups. The highest model efficiency was observed for the photochemical data obtained after 24h exposure to the water samples (91,1%) (Figure 7). This resulted from a maximum number of treatment groups displaying very high classification efficiencies. After this timepoint model overall classification reduced throughout exposure time, pulled down by lower group classification efficiencies, indicating a lower degree of dissimilarity between exposure groups, and thus a higher classification mismatch between sample groups.

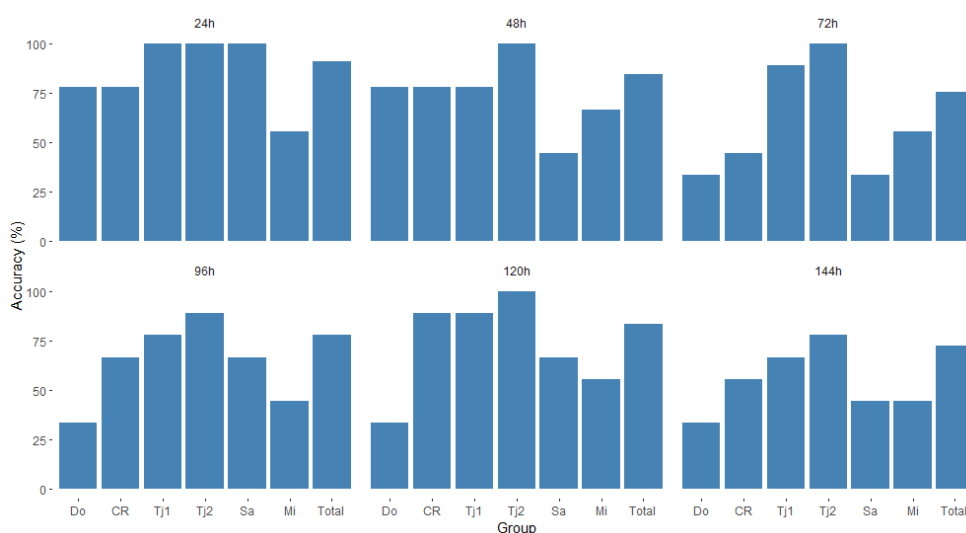


Figure 7. Canonical analysis of principal coordinates (CAP) classification accuracy between sites at each exposure timepoint (up to 144h) and model overall accuracy (Total).

The photo-physiological parameters derived from the OJIP Chlorophyll Fluorescence tests conducted on the diatoms showcased distinct and unique variations among the diatoms exposed to water samples from different sites. One of the said parameters, the Performance Index (PI) (Figure 8A), indicates diatoms in Sado to have the highest PI while diatoms from Tj2 has the lowest PI. Diatoms exposed to samples from Sado also displayed the lowest Dissipation per reaction center (Figure 8I). Diatoms from both Douro and Sado exposure achieved the highest SFI and the lowest SFI(NPQ) of all samples (Figure 8C, and 8D). Diatoms exposed to water from Tj2 had the lowest Performance Index. Diatoms exposed to Tj2 samples and Mira samples exhibited the lowest relative energy trappings and had a higher median dissipation than the rest (Figure 8F, 8I, and 8J). Diatoms exposed to water from Cabo Raso did not develop any unique photo-physiological characteristics, but, they showed more similarities to diatoms in Sado samples than diatoms in Tj2 samples. Diatoms in Cabo-Raso samples displayed higher PI, electron transfer (both relative and per reaction center), SFI, and lower SFI(NPQ) compared to Tj2 (Figure 8A, 8C, 8D, 8G, and 8H). On the other hand, Mira contrasts with Cabo Raso, as it shares more similarities with Tj2 for almost the exact parameters. Demonstrating lower PI, electron transfer (both relative and per reaction center), SFI, and higher relative and per reaction center dissipation and SFI(NPQ) than diatoms in Sado samples (Figure 8A, 8C, 8D, 8G, and 8H).

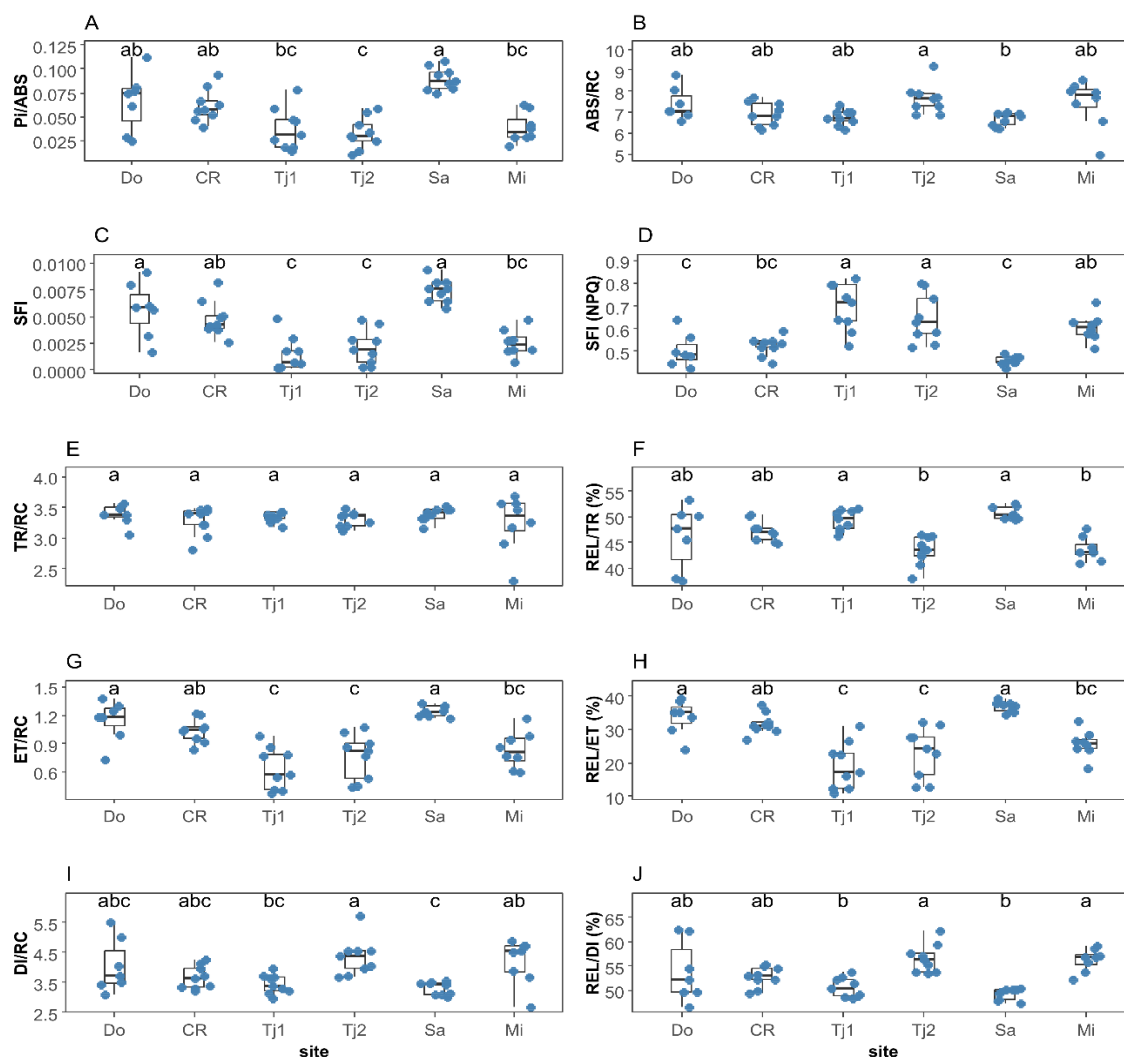


Figure 8. OJIP-derived physiological parameters ("PI"-Performance Index, "ABS/RC"-Absorbed energy flux per reaction center, "TRo/RC"-Trapped energy flux per reaction center, "TR(%)"-Relative Trapped energy flux normalized towards the absorbed energy flux $(TRo/RC)/(ABS/RC) \times 100$, "ETo/RC"-Transported energy flux per reaction center, "ET(%)"-Relative Transported energy flux normalized towards the trapped energy flux $(ETo/RC)/(TRo/RC) \times 100$, "DIo/RC"-Dissipated energy flux per reaction center, "DI(%)"-Relative Dissipated energy flux normalized towards the absorbed energy flux $(DIo/RC)/(ABS/RC) \times 100$, "SFI"-Structural and Functional Index of the Photochemical Reactions, "SFI (NPQ)" - Structural and Functional Index of the Non-Photochemical Reactions). Different letters denote significant differences at $p < 0.05$.

Analysing the correlation between pharmaceutical compounds and the photochemical traits evaluated in the exposed diatoms, it is possible to observe that most of the significant relationships are negative, thus indicating that increased pharmaceutical concentrations tend to decrease the assessed physiological parameters (Figure 9). The exception to this trend was SFI(NPQ), which exhibited positive correlations with pharmaceutical concentrations (Figure 9A). Notably, Indapamide, Carbamazepine, Acetaminophen, Sulfapyridine, and Venlafaxine had the most profound influence on ET, SFI, and SFI(NPQ). However, only Acetaminophen and Indapamide showed a significant negative correlation with the performance index. Flumequine was unique in its negative correlation with ET and no positive correlation with SFI(NPQ). However, both Losartan and Lorazepam exhibited a positive correlation with SFI(NPQ) without any negative correlation with ET. Notably, five pharmaceuticals, namely Alpha-Hydroxyalprazolam, Azithromycin, Ciprofloxacin, Sertraline, and Sulfamethoxazole, did not demonstrate significant

correlations with any of the tested physiological parameters (Figure 9A). The metals show few significant correlations with the photo-physiology, only lead (Pb) and titanium (Ti) had any correlations (Figure 9B). Both metals demonstrated positive correlations with the ABS/RC, DI/RC, and DI (%), while the only negative correlation was TR (%). The Risk Quotients (RQs) of the therapeutic groups are depicted in Figure 9C. The groups: analgesics, anxiolytics, NSAIDs, and lipid regulators, are comprised of a single pharmaceutical. Therefore, the correlation is equal to the RQ of their respective single-detected pharmaceuticals. Antibiotics did not show any significant correlation between RQs and photophysiological parameters, despite multiple antibiotics displaying correlations between their concentrations and the photophysiological traits assessed. Antidepressants and β -Blockers display the strongest correlations between RQ and Physiology (Figure 9C).

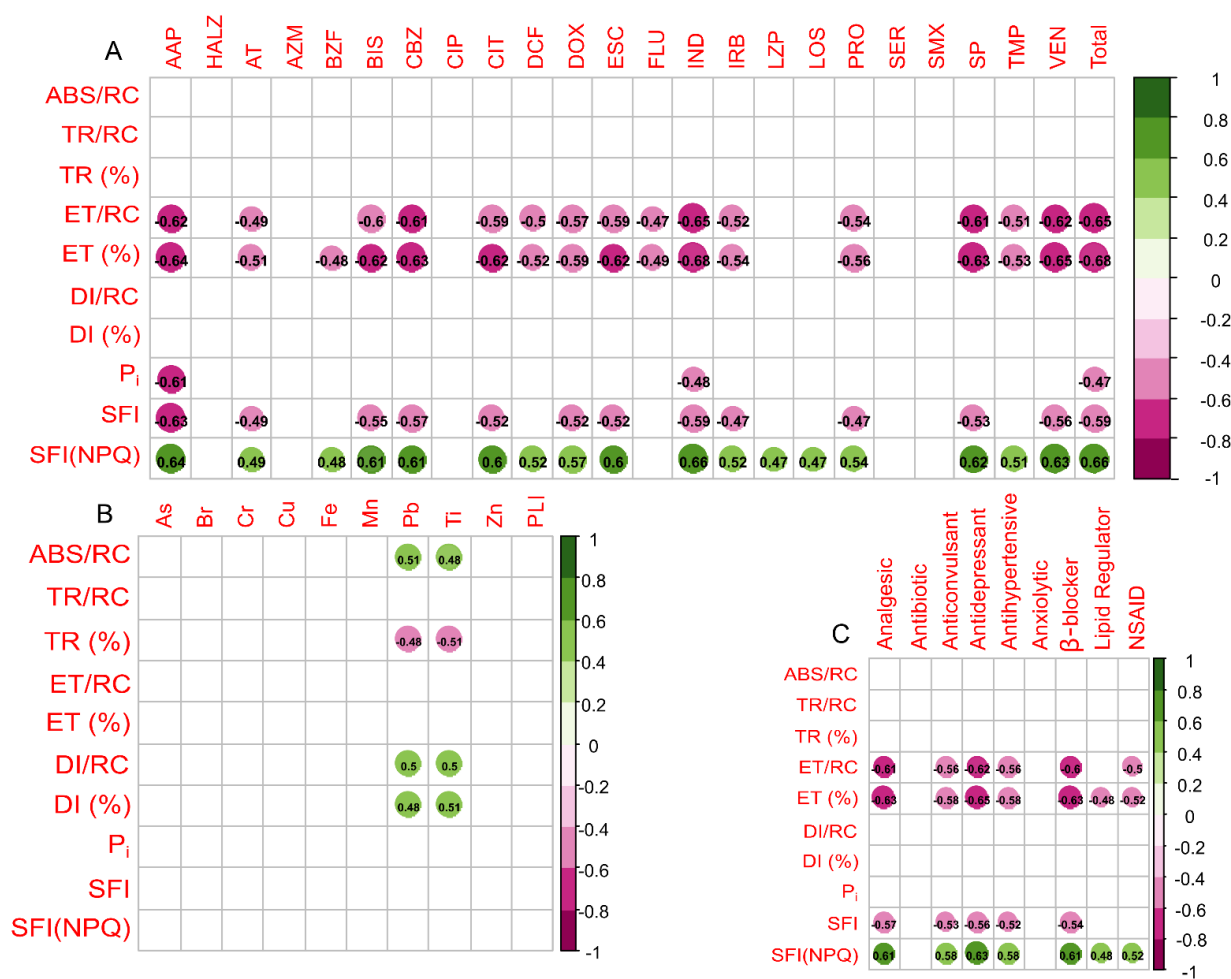


Figure 9. Spearman correlation coefficients (N=5) correlograms between photo-physiological parameters and pharmaceutical concentrations (A), metal concentrations (B) and the RQ (therapeutic group) (C). Positive correlations are represented in green and negative correlations in magenta. Only significant ($p < 0.05$) correlations are displayed. "AAP"-Acetaminophen, "AT"-Atenolol, "AZM"-Azithromycin, "BIS"-Bisoprolol, "BZF"-Bezafibrate, "CBZ"-Carbamazepine, "CIP"-Ciprofloxacin, "CIT"-Citalopram, "DCF"-Diclofenac, "DOX"-Doxycycline, "ESC"-Escitalopram, "FLU"-Flumequine, "HALZ"-Alpha-Hydroxyalprazolam, "IND"-Indapamide, "IRB"-Irbesartan, "LZP"-Lorazepam, "LOS"-Losartan "PRO"-Propranolol, "SER"-Sertraline, "SMX"-Sulfamethoxazole, "SP"-Sulfapyridine, "TMP"-Trimethoprim, "VEN"-Venlafaxine, "PI"-Performance Index, "ABS/RC"-Absorbed energy flux per reaction center, "TRo/RC"-Trapped energy flux per reaction center, "TR(%)"-Relative Trapped energy flux normalized towards the absorbed energy flux (TRo/RC)/(ABS/RC) x 100, "ETo/RC"-Transported energy flux per reaction center, "ET(%)"-Relative Transported energy flux normalized towards the trapped energy flux (ETo/RC)/(TRo/RC) x 100, "DIo/RC"-Dissipated energy flux per reaction center, "DI(%)"-Relative Dissipated energy flux normalized towards the absorbed energy flux (DIo/RC)/(ABS/RC) x 100, "SFI"-Structural and Functional Index of the Photochemical Reactions, "SFI (NPQ)"-Structural and Functional Index of the Non-Photochemical Reactions.

4. Discussion

The water chemical characterization based on both classic and emergent contaminants, namely metals and pharmaceuticals represent a comprehensive approach that better reflects environmental conditions. However, it's still important to reiterate that these are laboratory results. Testing *in situ* the method's ability to detect pharmaceutical contamination has yet to be evaluated (Cabrita et al., 2014). Additionally, it may provide other challenges, since pollutant and salt concentrations can vary greatly over time (Fonseca et al., 2020; Geyer & MacCready, 2014), therefore, further *in situ* testing is necessary. Additionally, since environmental concentrations of pharmaceuticals may exhibit a daily and seasonal variability that our sampling campaign was not designed for, further sampling covering this temporal variation of in Portugal's estuaries would provide valuable insights on the distribution patterns of these emergent pollutants.

The presence of pharmaceuticals was evident in all samples, and out of the 69 screened, only 23 were detected. The majority of the compounds detected belong to the antibiotics class, which is in line with previous studies that also report the prevalence of antibiotics in Europe (Zhou et al., 2019).

The sites located in the Tejo estuary, Tj1 and Tj2, consistently presented the highest concentrations per sample for multiple drugs. Four compounds – Bisoprolol, Irbesartan, Losartan, and Venlafaxine – were detected at levels considerably higher than those reported in 2021 (Fonseca et al., 2021). Nonetheless, it's important to mention that the maximum concentration of Venlafaxine detected may be atypical and could represent an isolated peak event. Prior studies have also reported peak concentrations of Carbamazepine exceeding the maximum detected concentration of Venlafaxine (Fonseca et al., 2021). Furthermore, a recent study (I. A. Duarte et al., 2023) supports this affirmation by reporting maximum values of Venlafaxine in the Tejo estuary within ranges similar to those in 2021. It's interesting to note that the peak was detected at both sampling stations in the Tejo estuary, specifically positioned to evaluate pharmaceuticals from wastewater treatment plants serving Lisbon and Almada urban areas. This synchronous surge may suggest the possibility of a shared event. Nonetheless, it is also important to note that pharmaceutical concentrations can vary greatly depending on site and seasonality (Letsinger et al., 2019).

Douro and Sado estuaries have not been the target of multiple comprehensive pharmaceutical assessments, but some of the detected compounds were previously detected in some works and can be used as a baseline. The pharmaceutical concentrations in the Douro estuary samples show a substantial decrease in comparison to the maximum levels reported in 2010 (Madureira et al., 2010), which report levels of Carbamazepine, Sulfamethoxazole, Trimethoprim, and Propranolol reaching a maximum value of 178 ng/L, 53.3 ng/L, 15.7 ng/L and 3.18 ng/L. However, in this study Carbamazepine, and Propranolol reached a maximum value in the Douro samples of 6.15 ng/L and 1.38 ng/L while Sulfamethoxazole and Trimethoprim were not detected. Another study in 2020 (Fernandes et al., 2020) also reported no detection of Trimethoprim and other pharmaceuticals, however, they appear with concentrations above LOD in our study (Azithromycin Carbamazepine Ciprofloxacin and Venlafaxine). The concentrations of the pharmaceuticals Citalopram, Sertraline and Venlafaxine in the Sado estuary were within previously described limits for this transitional system (I. A. Duarte et al., 2023), however, the majority of the available studies focus mainly on pesticides and endocrine-disrupting agents contamination (Ribeiro et al., 2009), reducing the amount of data available regarding pharmaceutical contamination in this system. The sites Mi (Mira) and CR (Cabo Raso) showed an increase in the detection of Azithromycin, Venlafaxine, and Propranolol when compared with

previous studies (Sousa et al., 2020). Additionally, considering the cumulative concentrations per water sample, some samples demonstrated higher concentrations than the detected in samples from Sado estuary. Overall the concentrations of pharmaceuticals detected align with those recorded in other water systems across Poland, Spain and UK (Letsinger et al., 2019; Mijangos et al., 2018; Ślósarczyk et al., 2021). Therefore, it is assumed that the patterns detected do not deviate from normal ranges found in other European regions.

The RQs obtained differ from other studies that consider concentrations across Europe. Zhou et al, (2019) categorized Diclofenac, Carbamazepine, and Venlafaxine as high risk, but, our results place them at a lower bracket (moderate to low risk). These discrepancies reflect regional variations and highlight the importance of local assessments before implementing measures.

Metal assessments tend to focus more on sediments rather than water concentrations since they provide more information regarding pollution trends and they can act as a historic reservoir for pollutants (García-Ordiales et al., 2020). However, water quality is intrinsically correlated to the concentration of pollutants present in the water column. While sediments can re-introduce metals into the water column through physical or biological disturbance (Atkinson et al., 2007), affecting the water quality and, by extension, the physiology of the diatom exposed to these metals. But with a Pollution Load index (PLI) of 0 across all samples it strengthens the idea that the main anthropogenic pressure that caused such physiological disparities is the pharmaceuticals. The metal concentrations were for the most part aligned with concentrations found in other European estuaries (Morillo et al., 2005; Radeva & Seymenov, 2021; Tzempelikou et al., 2021). However, the maximum arsenic concentration detected in the samples collected at Sado estuary was higher than in Spain's Odiel estuary (Morillo et al., 2005).

Even though the samples gathered from Tejo estuary (Tj1 and Tj2) demonstrate similar pollution levels, with an RQ above 1. The degree of their differences in photochemical traits (i.e., REL/TR, and relative and absolute dissipation) places them closer to diatom from other estuaries like Sado and Mira than from each other. This highlights the fact that the method is capable of sensing environmental shifts within estuaries, emphasizing its biomonitoring potential. Nonetheless, despite varying conditions, the fact that TRo/RC remained consistent throughout all test units also indicates that the overall trapping efficiency remained constant, highlighting the species' photosynthetic resilience.

Despite the diatoms exposed to Tj1 or Tj2 samples having statistically different dissipation rates, their SFI(NPQ) and SFI are similar. Suggesting that even though the two samples are managing their light energy differently, as indicated by the statistical difference in dissipation, the stressed cells' overall photosynthetic efficiency and their ability to manage light through SFI(NPQ) are similar.

The diatoms exposed to Douro or Sado samples developed very similar photo-physiological profiles. Notably, the samples from Sado have the lowest RQ and relatively low pollution level, which suggests that although the Douro water samples registered higher overall pollution levels in comparison to the Sado or Mira estuaries, the corresponding ecological risks posed might not be as severe.

While it can be hard to determine which pollutant, or combination thereof, is responsible for the disruption of specific metabolic pathways producing these results, it is important to highlight that these pollutants are indeed exerting clear signs of stress on the diatom as they would

in real environmental conditions were all contaminants interact with the organisms simultaneously.

The pollutant with the highest RQ was Losartan. According to (Godoy et al., 2015) a mixture of Losartan and Propranolol can lessen the effect of Losartan in green algae, and since all the samples containing Losartan also contain Propranolol it may be difficult to detect such effects. This is supported by the low set of significant correlations in Figure 9a.

The strong Spearman correlations between the antidepressants RQ and the photo-physiological parameters may be inflated due to the peak in Venlafaxine detected in some samples. The Spearman correlations also suggest some influence of lead (Pb) and titanium (Ti) on diatom physiology, leading to increases in both absorbed and dissipated energy flux while decreasing the trapped energy flux of the exposed diatoms. Lead concentrations, concomitant increased values in the dissipation energy flux and decreased trapping energy flux may hint towards slight growth inhibition. This result is in line with previous research on lead effects in *P. tricornutum* (Cabrita et al., 2018). The correlations suggest that pharmaceuticals and metals affect algal physiology differently. As the general concentration of pharmaceuticals increases, so does the structural and functional index for the non-photochemical reactions (SFI(NPQ)), whereas the transport energy flux and the structural and functional index (SFI) occasionally force the performance index to decrease. Other studies have also reported that increased pharmaceutical concentrations can weaken the photosynthetic cycle by inducing lower light energy absorption, lower electron transfer and trapping capacity and higher dissipation (Mao et al., 2021). Consequently, the inhibition of the electron transport chain can induce the generation of reactive oxygen species (ROS) due to excessive accumulation of redox potential and lead to oxidative damage (Mao et al., 2021). However, no correlations with the dissipated energy flux were found in our results, suggesting energetic reallocation. For the metals, the increase in the absorbed and dissipation energy fluxes, coupled with a reduction in trapping energy flux, are clear signs that these elements are related to the stress signs observed.

By optically analysing the differences in the physiological state of immobilized *P. tricornutum* at each site under different anthropogenic pressures, it becomes evident that it is possible to perform a cost-effective and daily ongoing analysis resorting to this methodology. Incomplete treatment of wastewater can influence the overall water quality and due to the bioactive nature of these pollutants, also affect wildlife (Gunnarsson et al., 2008). Since reducing the quantity of pharmaceuticals taken is not an option, the burden of responsibility lies with wastewater treatment plants. However, the implementation of more modern systems or the adjustment of existing ones is a costly procedure. According to a recent study, upgrading all waste water treatment plants in England to be capable of maintaining a flow of synthetic estrogens that complies with EU regulations would cost an estimated 28 billion Euros (Ford & Herrera, 2019). Another possible mitigation tactic may lie with a change in population behaviour, as the implementation of widely available “take back” programs may decrease the number of pharmaceuticals that enter aquatic systems directly (Ford & Herrera, 2019). Monitoring and understanding the effect compounds like pharmaceuticals or trace metals can have on fauna and flora is paramount to maintaining a stable and biodiverse estuarine or coastal ecosystem. The destabilization of phytoplankton populations through water contamination can have cascading effects throughout the trophic web (Biemyer-Fraser et al., 2014). Additionally, the bioamplification of pharmaceuticals or their metabolites can detrimentally impact wildlife through changes in reproductive or behavioural patterns (Corcoran et al., 2010).

Estuaries play a vital role, as feeding grounds and nurseries, in the life cycle of many marine species. However, these vulnerable life stages could be disproportionately impacted by contaminants (Monteiro et al., 2007). Additionally, a degraded estuary, compromised by pollution, may deter human activity, leading to negative socioeconomic consequences for coastal communities and ecosystems alike (Angradi et al., 2016).

Conclusion

The contamination levels detected highlight the need for better wastewater treatment and the need for more environmental risk assessments to better monitor these pollutants. However, given the financial weight required for the former as highlighted by Ford and Herrera, (2019), it becomes clear the need for cost-effective alternatives. This study affirms the proposed method for monitoring relative water quality using immobilized *P. tricornutum* as a viable cost-effective option. The experimental design accounts for some of the natural fluctuation of concentrations between sites and demonstrated the effectiveness of analysing the photo-physiological parameters of *P. tricornutum* as a biomonitoring tool, since the immobilization technique didn't hinder either the diatom's ability to react to environmental pressures or the detection of fluorescence emitted from the diatom. Due to its low protocol cost and "passive" nature, it is possible to manage a higher number of testing stations and increase the definition (or size) of the study area depending on the type of study. While distinguishing between individual pollutants is inherently difficult in mixture exposure trials, in environmental conditions pollutants are present in mixtures. Thus, the presented testing design and the results obtained can better recreate actual true scenarios. The long-term health and sustainability of estuaries are intrinsically related to overall water quality (Araujo et al., 2017). Monitoring water quality is crucial for the timely detection of pollution hotspots, enabling the swift implementation of appropriate environmental measures, ensuring the habitat maintains its capacity.

The ecological significance of estuaries as feeding grounds and nurseries for marine species cannot be overstated. Preserving these habitats from contamination is crucial for maintaining biodiversity and sustaining coastal ecosystems, therefore, marine conservation efforts should reflect this importance. The collection of environmental data is a cornerstone of informed decision-making, for without it, it's impossible to accurately assess the state of ecosystems and implement the necessary measures.

6. References

- Able, K. W. (2005). A re-examination of fish estuarine dependence: Evidence for connectivity between estuarine and ocean habitats. *Estuarine, Coastal and Shelf Science*, *64*(1), 5–17. <https://doi.org/10.1016/j.ecss.2005.02.002>
- Angradi, T. R., Launspach, J. J., Bolgrien, D. W., Bellinger, B. J., Starry, M. A., Hoffman, J. C., Trebitz, A. S., Sierszen, M. E., & Hollenhorst, T. P. (2016). Mapping ecosystem service indicators in a Great Lakes estuarine Area of Concern. *Journal of Great Lakes Research*, *42*(3), 717–727. <https://doi.org/10.1016/j.jglr.2016.03.012>
- Araujo, A. V., Dias, C. O., & Bonecker, S. L. C. (2017). Effects of environmental and water quality parameters on the functioning of copepod assemblages in tropical estuaries. *Estuarine, Coastal and Shelf Science*, *194*, 150–161. <https://doi.org/10.1016/j.ecss.2017.06.014>
- Atkinson, C. A., Jolley, D. F., & Simpson, S. L. (2007). Effect of overlying water pH, dissolved oxygen, salinity and sediment disturbances on metal release and sequestration from metal contaminated marine sediments. *Chemosphere*, *69*(9), 1428–1437. <https://doi.org/10.1016/j.chemosphere.2007.04.068>
- Backhaus, T., & Faust, M. (2012). Predictive environmental risk assessment of chemical mixtures: A conceptual framework. *Environmental Science & Technology*, *46*(5), 2564–2573. <https://doi.org/10.1021/es2034125>
- Beck, M. W., Heck, K. L., Able, K. W., Childers, D. L., Eggleston, D. B., Gillanders, B. M., Halpern, B., Hays, C. G., Hoshino, K., Minello, T. J., Orth, R. J., Sheridan, P. F., & Weinstein, M. P. (2001). The Identification, Conservation, and Management of Estuarine and Marine Nurseries for Fish and Invertebrates: A better understanding of the habitats that serve as nurseries for marine species and the factors that create site-specific variability in nursery quality will improve conservation and management of these areas. *BioScience*, *51*(8), 633–641. [https://doi.org/10.1641/0006-3568\(2001\)051\[0633:TICAMO\]2.0.CO;2](https://doi.org/10.1641/0006-3568(2001)051[0633:TICAMO]2.0.CO;2)

- Bielmyer-Fraser, G. K., Jarvis, T. A., Lenihan, H. S., & Miller, R. J. (2014). Cellular partitioning of nanoparticulate versus dissolved metals in marine phytoplankton. *Environmental Science & Technology*, 48(22), 13443–13450. <https://doi.org/10.1021/es501187g>
- Branchet, P., Arpin-Pont, L., Piram, A., Boissery, P., Wong-Wah-Chung, P., & Doumenq, P. (2021). Pharmaceuticals in the marine environment: What are the present challenges in their monitoring? *Science of The Total Environment*, 766, 142644. <https://doi.org/10.1016/j.scitotenv.2020.142644>
- Cabrita, M. T., Duarte, B., Gameiro, C., Godinho, R. M., & Caçador, I. (2018). Photochemical features and trace element substituted chlorophylls as early detection biomarkers of metal exposure in the model diatom *Phaeodactylum tricornutum*. *Ecological Indicators*, 95, 1038–1052. <https://doi.org/10.1016/j.ecolind.2017.07.057>
- Cabrita, M. T., Raimundo, J., Pereira, P., & Vale, C. (2013). Optimizing alginate beads for the immobilisation of *Phaeodactylum tricornutum* in estuarine waters. *Marine Environmental Research*, 87–88, 37–43. <https://doi.org/10.1016/j.marenvres.2013.03.002>
- Cabrita, M. T., Raimundo, J., Pereira, P., & Vale, C. (2014). Immobilised *Phaeodactylum tricornutum* as biomonitor of trace element availability in the water column during dredging. *Environmental Science and Pollution Research*, 21(5), 3572–3581. <https://doi.org/10.1007/s11356-013-2362-x>
- Ceschin, S., Bellini, A., & Scalici, M. (2021). Aquatic plants and ecotoxicological assessment in freshwater ecosystems: A review. *Environmental Science and Pollution Research*, 28(5), 4975–4988. <https://doi.org/10.1007/s11356-020-11496-3>
- Chau, H. T. C., Kadokami, K., Ifuku, T., & Yoshida, Y. (2017). Development of a comprehensive screening method for more than 300 organic chemicals in water samples using a combination of solid-phase extraction and liquid chromatography-time-of-flight-mass

- spectrometry. *Environmental Science and Pollution Research*, 24(34), 26396–26409.
<https://doi.org/10.1007/s11356-017-9929-x>
- Corcoran, J., Winter, M. J., & Tyler, C. R. (2010). Pharmaceuticals in the aquatic environment: A critical review of the evidence for health effects in fish. *Critical Reviews in Toxicology*, 40(4), 287–304. <https://doi.org/10.3109/10408440903373590>
- Cruz de Carvalho, R., Feijão, E., Matos, A. R., Cabrita, M. T., Novais, S. C., Lemos, M. F. L., Caçador, I., Marques, J. C., Reis-Santos, P., Fonseca, V. F., & Duarte, B. (2020). Glyphosate-Based Herbicide Toxicophenomics in Marine Diatoms: Impacts on Primary Production and Physiological Fitness. *Applied Sciences*, 10(21), Article 21.
<https://doi.org/10.3390/app10217391>
- D’Alessio, M., Yoneyama, B., & Ray, C. (2015). Fate of selected pharmaceutically active compounds during simulated riverbank filtration. *Science of The Total Environment*, 505, 615–622. <https://doi.org/10.1016/j.scitotenv.2014.10.032>
- de Oliveira, L. L. D., Antunes, S. C., Gonçalves, F., Rocha, O., & Nunes, B. (2016). Acute and chronic ecotoxicological effects of four pharmaceuticals drugs on cladoceran *Daphnia magna*. *Drug and Chemical Toxicology*, 39(1), 13–21.
<https://doi.org/10.3109/01480545.2015.1029048>
- Duarte, B., Duarte, I. A., Caçador, I., Reis-Santos, P., Vasconcelos, R. P., Gameiro, C., Tanner, S. E., & Fonseca, V. F. (2022). Elemental fingerprinting of thornback ray (*Raja Clavata*) muscle tissue as a tracer for provenance and food safety assessment. *Food Control*, 133, 108592. <https://doi.org/10.1016/j.foodcont.2021.108592>
- Duarte, B., Feijão, E., Cruz de Carvalho, R., Duarte, I. A., Marques, A. P., Maia, M., Hertzog, J., Matos, A. R., Cabrita, M. T., & Caçador, I. (2022). Untargeted Metabolomics Reveals Antidepressant Effects in a Marine Photosynthetic Organism: The Diatom *Phaeodactylum tricornutum* as a Case Study. *Biology*, 11(12), 1770.
<https://doi.org/10.3390/biology11121770>

- Duarte, B., Feijão, E., Cruz de Carvalho, R., Franzitta, M., Carlos Marques, J., Caçador, I., Teresa Cabrita, M., & Fonseca, V. F. (2021). Unlocking Kautsky's dark box: Development of an optical toxicity classification tool (OPTOX index) with marine diatoms exposed to emerging contaminants. *Ecological Indicators*, *131*, 108238.
<https://doi.org/10.1016/j.ecolind.2021.108238>
- Duarte, B., Gameiro, C., Utkin, A. B., Matos, A. R., Caçador, I., Fonseca, V., & Cabrita, M. T. (2021). A multivariate approach to chlorophyll a fluorescence data for trace element ecotoxicological trials using a model marine diatom. *Estuarine, Coastal and Shelf Science*, *250*, 107170. <https://doi.org/10.1016/j.ecss.2021.107170>
- Duarte, B., Prata, D., Matos, A. R., Cabrita, M. T., Caçador, I., Marques, J. C., Cabral, H. N., Reis-Santos, P., & Fonseca, V. F. (2019). Ecotoxicity of the lipid-lowering drug bezafibrate on the bioenergetics and lipid metabolism of the diatom *Phaeodactylum tricornutum*. *Science of The Total Environment*, *650*, 2085–2094.
<https://doi.org/10.1016/j.scitotenv.2018.09.354>
- Duarte, I. A., Reis-Santos, P., Fick, J., Cabral, H. N., Duarte, B., & Fonseca, V. F. (2023). Neuroactive pharmaceuticals in estuaries: Occurrence and tissue-specific bioaccumulation in multiple fish species. *Environmental Pollution*, *316*, 120531.
<https://doi.org/10.1016/j.envpol.2022.120531>
- ECHA. (2003). *Technical Guidance Document on Risk Assessment Part II, European Commission*. European Chemicals Agency, 2012.
https://echa.europa.eu/documents/10162/987906/tgdpart2_2ed_en.pdf/138b7b71-a069-428e-9036-62f4300b752f
- ECHA. (2008). *Guidance on information requirements and chemical safety assessment Part D: Exposure Scenario Building*. European Chemicals Agency, 2012.
<https://echa.europa.eu/guidance-documents/guidance-on-information-requirements-and-chemical-safety-assessment>

- ECOSAR. (2012). Methodology document for the ecological structure-activity relationship model (ECOSAR) class program. *US-EPA, Washington DC*, 46.
- Faafeng, B., van Donk, E., & Källqvist, S. T. (1994). In situ measurement of algal growth potential in aquatic ecosystems by immobilized algae. *Journal of Applied Phycology*, 6(3), 301–308.
- Feijão, E., Gameiro, C., Franzitta, M., Duarte, B., Caçador, I., Cabrita, M. T., & Matos, A. R. (2018). Heat wave impacts on the model diatom *Phaeodactylum tricornutum*: Searching for photochemical and fatty acid biomarkers of thermal stress. *Ecological Indicators*, 95, 1026–1037. <https://doi.org/10.1016/j.ecolind.2017.07.058>
- Fernandes, M. J., Paíga, P., Silva, A., Llaguno, C. P., Carvalho, M., Vázquez, F. M., & Delerue-Matos, C. (2020). Antibiotics and antidepressants occurrence in surface waters and sediments collected in the north of Portugal. *Chemosphere*, 239, 124729. <https://doi.org/10.1016/j.chemosphere.2019.124729>
- Fonseca, V. F., Duarte, I. A., Duarte, B., Freitas, A., Pouca, A. S. V., Barbosa, J., Gillanders, B. M., & Reis-Santos, P. (2021). Environmental risk assessment and bioaccumulation of pharmaceuticals in a large urbanized estuary. *Science of The Total Environment*, 783, 147021. <https://doi.org/10.1016/j.scitotenv.2021.147021>
- Fonseca, V. F., Reis-Santos, P., Duarte, B., Cabral, H. N., Caçador, M. I., Vaz, N., Dias, J. M., & Pais, M. P. (2020). Roving pharmacies: Modelling the dispersion of pharmaceutical contamination in estuaries. *Ecological Indicators*, 115, 106437. <https://doi.org/10.1016/j.ecolind.2020.106437>
- Ford, A. T., & Herrera, H. (2019). ‘Prescribing’ psychotropic medication to our rivers and estuaries. *BJPsych Bulletin*, 43(4), 147–150. <https://doi.org/10.1192/bjb.2018.72>
- Freitas, A., Leston, S., Rosa, J., Castilho, M. da C., Barbosa, J., Rema, P., Pardal, M. Â., & Ramos, F. (2014). Multi-residue and multi-class determination of antibiotics in gilthead sea bream (*Sparus aurata*) by ultra high-performance liquid chromatography-tandem mass

- spectrometry. *Food Additives & Contaminants: Part A*, 31(5), 817–826.
<https://doi.org/10.1080/19440049.2014.891764>
- García-Ordiales, E., Flor-Blanco, G., Roqueñí, N., Covelli, S., Cienfuegos, P., Álvarez, R., Fontolan, G., & Loredó, J. (2020). Anthropocene footprint in the Nalón estuarine sediments (northern Spain). *Marine Geology*, 424, 106167.
<https://doi.org/10.1016/j.margeo.2020.106167>
- Garzke, J., Connor, S. J., Sommer, U., & O'Connor, M. I. (2019). Trophic interactions modify the temperature dependence of community biomass and ecosystem function. *PLOS Biology*, 17(6), e2006806. <https://doi.org/10.1371/journal.pbio.2006806>
- Gaw, S., Thomas, K. V., & Hutchinson, T. H. (2014). Sources, impacts and trends of pharmaceuticals in the marine and coastal environment. *Philosophical Transactions of the Royal Society B: Biological Sciences*, 369(1656), 20130572.
<https://doi.org/10.1098/rstb.2013.0572>
- Geyer, W. R., & MacCready, P. (2014). The Estuarine Circulation. *Annual Review of Fluid Mechanics*, 46(1), 175–197. <https://doi.org/10.1146/annurev-fluid-010313-141302>
- Gillanders, B. M., Able, K. W., Brown, J. A., Eggleston, D. B., & Sheridan, P. F. (2003). Evidence of connectivity between juvenile and adult habitats for mobile marine fauna: An important component of nurseries. *Marine Ecology Progress Series*, 247, 281–295.
<https://doi.org/10.3354/meps247281>
- Gunnarsson, L., Jauhiainen, A., Kristiansson, E., Nerman, O., & Larsson, D. G. J. (2008). Evolutionary Conservation of Human Drug Targets in Organisms used for Environmental Risk Assessments. *Environmental Science & Technology*, 42(15), 5807–5813. <https://doi.org/10.1021/es8005173>
- Hernando, M. D., Mezcuá, M., Fernández-Alba, A. R., & Barceló, D. (2006). Environmental risk assessment of pharmaceutical residues in wastewater effluents, surface waters and sediments. *Talanta*, 69(2), 334–342. <https://doi.org/10.1016/j.talanta.2005.09.037>

- Hicks, K. A., Fuzzen, M. L. M., McCann, E. K., Arlos, M. J., Bragg, L. M., Kleywegt, S., Tetreault, G. R., McMaster, M. E., & Servos, M. R. (2017). Reduction of Intersex in a Wild Fish Population in Response to Major Municipal Wastewater Treatment Plant Upgrades. *Environmental Science & Technology*, *51*(3), 1811–1819.
<https://doi.org/10.1021/acs.est.6b05370>
- Kaiser, D., Kowalski, N., Böttcher, M. E., Yan, B., & Unger, D. (2015). Benthic Nutrient Fluxes from Mangrove Sediments of an Anthropogenically Impacted Estuary in Southern China. *Journal of Marine Science and Engineering*, *3*(2), Article 2.
<https://doi.org/10.3390/jmse3020466>
- Küster, A., & Adler, N. (2014). Pharmaceuticals in the environment: Scientific evidence of risks and its regulation. *Philosophical Transactions of the Royal Society B: Biological Sciences*, *369*(1656), 20130587. <https://doi.org/10.1098/rstb.2013.0587>
- Lenanton, R. C. J., & Potter, I. C. (1987). Contribution of estuaries to commercial fisheries in temperate Western Australia and the concept of estuarine dependence. *Estuaries*, *10*(1), 28–35. <https://doi.org/10.2307/1352022>
- Letsinger, S., Kay, P., Rodríguez-Mozaz, S., Villagrassa, M., Barceló, D., & Rotchell, J. M. (2019). Spatial and temporal occurrence of pharmaceuticals in UK estuaries. *Science of The Total Environment*, *678*, 74–84. <https://doi.org/10.1016/j.scitotenv.2019.04.182>
- Levin, L. A., Boesch, D. F., Covich, A., Dahm, C., Erséus, C., Ewel, K. C., Kneib, R. T., Moldenke, A., Palmer, M. A., Snelgrove, P., Strayer, D., & Weslawski, J. M. (2001). The Function of Marine Critical Transition Zones and the Importance of Sediment Biodiversity. *Ecosystems*, *4*(5), 430–451. <https://doi.org/10.1007/s10021-001-0021-4>
- Lewis, M. A. (1995). Use of freshwater plants for phytotoxicity testing: A review. *Environmental Pollution*, *87*(3), 319–336. [https://doi.org/10.1016/0269-7491\(94\)P4164-J](https://doi.org/10.1016/0269-7491(94)P4164-J)

- Lopes, D. G., Duarte, I. A., Antunes, M., & Fonseca, V. F. (2020). Effects of antidepressants in the reproduction of aquatic organisms: A meta-analysis. *Aquatic Toxicology*, 227, 105569. <https://doi.org/10.1016/j.aquatox.2020.105569>
- Lytle, J. S., & Lytle, T. F. (2001). Use of plants for toxicity assessment of estuarine ecosystems. *Environmental Toxicology and Chemistry*, 20(1), 68–83. <https://doi.org/10.1002/etc.5620200107>
- Madureira, T. V., Barreiro, J. C., Rocha, M. J., Rocha, E., Cass, Q. B., & Tiritan, M. E. (2010). Spatiotemporal distribution of pharmaceuticals in the Douro River estuary (Portugal). *Science of The Total Environment*, 408(22), 5513–5520. <https://doi.org/10.1016/j.scitotenv.2010.07.069>
- Mao, Y., Yu, Y., Ma, Z., Li, H., Yu, W., Cao, L., & He, Q. (2021). Azithromycin induces dual effects on microalgae: Roles of photosynthetic damage and oxidative stress. *Ecotoxicology and Environmental Safety*, 222, 112496. <https://doi.org/10.1016/j.ecoenv.2021.112496>
- Mijangos, L., Ziarrusta, H., Ros, O., Kortazar, L., Fernández, L. A., Olivares, M., Zuloaga, O., Prieto, A., & Etxebarria, N. (2018). Occurrence of emerging pollutants in estuaries of the Basque Country: Analysis of sources and distribution, and assessment of the environmental risk. *Water Research*, 147, 152–163. <https://doi.org/10.1016/j.watres.2018.09.033>
- Minguez, L., Pedelucq, J., Farcy, E., Ballandonne, C., Budzinski, H., & Halm-Lemeille, M.-P. (2016). Toxicities of 48 pharmaceuticals and their freshwater and marine environmental assessment in northwestern France. *Environmental Science and Pollution Research*, 23(6), 4992–5001. <https://doi.org/10.1007/s11356-014-3662-5>
- Monteiro, M., Quintaneiro, C., Nogueira, A. J. A., Morgado, F., Soares, A. M. V. M., & Guilhermino, L. (2007). Impact of chemical exposure on the fish *Pomatoschistus*

- microps* Krøyer (1838) in estuaries of the Portuguese Northwest coast. *Chemosphere*, 66(3), 514–522. <https://doi.org/10.1016/j.chemosphere.2006.05.061>
- Moreira, S. M., Moreira-Santos, M., Guilhermino, L., & Ribeiro, R. (2006). Immobilization of the marine microalga *Phaeodactylum tricornutum* in alginate for in situ experiments: Bead stability and suitability. *Enzyme and Microbial Technology*, 38(1–2), 135–141. <https://doi.org/10.1016/j.enzmictec.2005.05.005>
- Moreira-Santos, M., Soares, A. M., & Ribeiro, R. (2004). A phytoplankton growth assay for routine in situ environmental assessments. *Environmental Toxicology and Chemistry: An International Journal*, 23(6), 1549–1560. <https://doi.org/10.1897/03-389>
- Morillo, J., Usero, J., & Gracia, I. (2005). Biomonitoring of trace metals in a mine-polluted estuarine system (Spain). *Chemosphere*, 58(10), 1421–1430. <https://doi.org/10.1016/j.chemosphere.2004.09.093>
- Nie, X.-P., Liu, B.-Y., Yu, H.-J., Liu, W.-Q., & Yang, Y.-F. (2013). Toxic effects of erythromycin, ciprofloxacin and sulfamethoxazole exposure to the antioxidant system in *Pseudokirchneriella subcapitata*. *Environmental Pollution*, 172, 23–32. <https://doi.org/10.1016/j.envpol.2012.08.013>
- Pal, A., He, Y., Jekel, M., Reinhard, M., & Gin, K. Y.-H. (2014). Emerging contaminants of public health significance as water quality indicator compounds in the urban water cycle. *Environment International*, 71, 46–62. <https://doi.org/10.1016/j.envint.2014.05.025>
- Petrović, M., Hernando, M. D., Díaz-Cruz, M. S., & Barceló, D. (2005). Liquid chromatography–tandem mass spectrometry for the analysis of pharmaceutical residues in environmental samples: A review. *Journal of Chromatography A*, 1067(1), 1–14. <https://doi.org/10.1016/j.chroma.2004.10.110>
- R Core Team. (2022). *R: A language and environment for statistical computing* [Computer software]. R Foundation for Statistical Computing. <https://www.R-project.org/>

- Radeva, K., & Seymenov, K. (2021). Surface water pollution with nutrient components, trace metals and metalloids in agricultural and mining-affected river catchments: A case study for three tributaries of the Maritsa River, Southern Bulgaria. *Geographica Pannonica*, 25(3), 214–225. <https://doi.org/10.5937/gp25-30811>
- Radomirović, M., Ćirović, Ž., Maksin, D., Bakić, T., Lukić, J., Stanković, S., & Onjia, A. (2020). Ecological Risk Assessment of Heavy Metals in the Soil at a Former Painting Industry Facility. *Frontiers in Environmental Science*, 8, 560415. <https://doi.org/10.3389/fenvs.2020.560415>
- Renzi, M., Roselli, L., Giovani, A., Focardi, S. E., & Basset, A. (2014). Early warning tools for ecotoxicity assessment based on *Phaeodactylum tricornutum*. *Ecotoxicology*, 23(6), 1055–1072. <https://doi.org/10.1007/s10646-014-1249-z>
- Ribeiro, C., Pardal, M. Â., Tiritan, M. E., Rocha, E., Margalho, R. M., & Rocha, M. J. (2009). Spatial distribution and quantification of endocrine-disrupting chemicals in Sado River estuary, Portugal. *Environmental Monitoring and Assessment*, 159(1), 415–427. <https://doi.org/10.1007/s10661-008-0639-1>
- Ringwood, A. H., & Keppler, C. J. (2002). Water quality variation and clam growth: Is pH really a non-issue in estuaries? *Estuaries*, 25(5), 901–907. <https://doi.org/10.1007/BF02691338>
- Riva, F., Zuccato, E., Davoli, E., Fattore, E., & Castiglioni, S. (2019). Risk assessment of a mixture of emerging contaminants in surface water in a highly urbanized area in Italy. *Journal of Hazardous Materials*, 361, 103–110. <https://doi.org/10.1016/j.jhazmat.2018.07.099>
- Santos, L., Soares, B., Rosa, J., Freitas, A., Leston, S., Barbosa, J., & Ramos, F. (2016). Detection and Quantification of 41 Antibiotic Residues in Gilthead Sea Bream (*Sparus aurata*) From Aquaculture Origin, Using a Multiclass and Multi-residue UHPLC-MS/MS Method. *Food Analytical Methods*, 9(10), 2749–2753. <https://doi.org/10.1007/s12161-016-0462-1>

- Santos, M. M. D., Moreno-Garrido, I., Gonçalves, F., Soares, A. M. V. M., & Ribeiro, R. (2002). An in situ bioassay for estuarine environments using the microalga *Phaeodactylum tricornutum*. *Environmental Toxicology and Chemistry: An International Journal*, 21(3), 567–574. <https://doi.org/10.1002/etc.5620210315>
- SCHER, SCCS, SCENIHR. (2012). *Toxicity and assessment of chemical mixtures*. Publications Office of the European Union. <https://data.europa.eu/doi/10.2772/21444>
- Ślósarczyk, K., Jakóbczyk-Karpierz, S., Rózkowski, J., & Witkowski, A. J. (2021). Occurrence of Pharmaceuticals and Personal Care Products in the Water Environment of Poland: A Review. *Water*, 13(16), Article 16. <https://doi.org/10.3390/w13162283>
- Sousa, J. C. G., Barbosa, M. O., Ribeiro, A. R. L., Ratola, N., Pereira, M. F. R., & Silva, A. M. T. (2020). Distribution of micropollutants in estuarine and sea water along the Portuguese coast. *Marine Pollution Bulletin*, 154, 111120. <https://doi.org/10.1016/j.marpolbul.2020.111120>
- Tomlinson, D. L., Wilson, J. G., Harris, C. R., & Jeffrey, D. W. (1980). Problems in the assessment of heavy-metal levels in estuaries and the formation of a pollution index. *Helgoländer Meeresuntersuchungen*, 33(1), 566–575. <https://doi.org/10.1007/BF02414780>
- Tzempelikou, E., Zeri, C., Iliakis, S., & Paraskevopoulou, V. (2021). Cd, Co, Cu, Ni, Pb, Zn in coastal and transitional waters of Greece and assessment of background concentrations: Results from 6 years implementation of the Water Framework Directive. *Science of The Total Environment*, 774, 145177. <https://doi.org/10.1016/j.scitotenv.2021.145177>
- Vasconcelos, R. P., Reis-Santos, P., Fonseca, V., Maia, A., Ruano, M., França, S., Vinagre, C., Costa, M. J., & Cabral, H. (2007). Assessing anthropogenic pressures on estuarine fish nurseries along the Portuguese coast: A multi-metric index and conceptual approach. *Science of The Total Environment*, 374(2–3), 199–215. <https://doi.org/10.1016/j.scitotenv.2006.12.048>

WOA. (2021). *The Second World Ocean Assessment, United Nations: Vol. II*

(<https://www.un.org/regularprocess/sites/www.un.org.regularprocess/files/2011859-e-woa-ii-vol-ii.pdf>).

<https://www.un.org/regularprocess/sites/www.un.org.regularprocess/files/2011859-e-woa-ii-vol-ii.pdf>

Zhou, S., Di Paolo, C., Wu, X., Shao, Y., Seiler, T.-B., & Hollert, H. (2019). Optimization of screening-level risk assessment and priority selection of emerging pollutants – The case of pharmaceuticals in European surface waters. *Environment International*, 128, 1–10. <https://doi.org/10.1016/j.envint.2019.04.034>

Zhu, X.-G., Govindjee, Baker, N. R., deSturler, E., Ort, D. R., & Long, S. P. (2005). Chlorophyll a fluorescence induction kinetics in leaves predicted from a model describing each discrete step of excitation energy and electron transfer associated with Photosystem II. *Planta*, 223(1), 114–133. <https://doi.org/10.1007/s00425-005-0064-4>

7. Supplements

Table supplement 1. List of the 69 compounds screened

Therapeutic group	Pharmaceutical
Anticonvulsant	
1	Carbamazepine
2	Gabapentin
3	Topiramate
Anxiolytics	
4	Alprazolam
5	Lorazepam
Antidepressants	
6	Citalopram
7	Escitalopram
8	Fluoxetine
9	Sertraline
10	Venlafaxine
Lipid-Regulators	
11	Atorvastatin
12	Bezafibrate
13	Fenofibrate
14	Gemfibrozil
15	Simvastatin
Nonsteroidal anti-inflammatory drugs (NSAID)	
16	Diclofenac
17	Ibuprofen
18	Nimesulide
19	Acetaminophen
Antihypertensive	
20	Furosemide
21	Indapamide
22	Irbesartan
23	Losartan
β -blocker	
24	Atenolol
25	Bisoprolol
26	Carvedilol
27	Propranolol
Antipsychotics	
28	Clozapine
Antibiotics	
29	Amoxicillin
30	Azithromycin
31	Benzylpenicillin
32	Ceftiofur
33	Cephalexin
34	Chlortetracycline

35	Cinoxacin
36	Ciprofloxacin
37	Danofloxacin
38	Doxicicline
39	Enoxacin
40	Enrofloxacin
41	Epi-chlortetracycline
42	Epi-tetracycline
43	Erythromycin
44	Flumequine
45	Marbofloxacin
46	Nalidixic acid
47	Norfloxacin
48	Ofloxacin
49	Oxacillin
50	Oxitetracline
51	Oxolinic acid
52	Spiramycin
53	Sulfachloropyridazine
54	Sulfadiazine
55	Sulfadimethoxine
56	Sulfadoxine
57	Sulfamethazine
58	Sulfamethizole
59	Sulfamethoxazole
60	Sulfanilamide
61	Sulfapyridine
62	Sulfaquinoxaline
63	Sulfathiazole
64	Sulfisomidine
65	Sulfisoxazole
66	Tetracycline
67	Tilmicosin
68	Trimethoprim
69	Tylosin

Table supplement 2. Limits of detection (LOD) of the 23 pharmaceuticals detected

Therapeutic group	Pharmaceutical	LOD (ng/L)
Analgesic	Acetaminophen	1,89
Anxiolytic	Alpha-Hydroxyalprazolam	0,02
NSAID	Diclofenac	0,02
Lipid-Regulator	Bezafibrate	0,07
Anticonvulsant	Carbamazepine	0,01
	Lorazepam	2,98
β -blocker	Atenolol	0,01
	Bisoprolol	0,14
	Propranolol	0,06
Antibiotic	Azithromycin	0,01
	Ciprofloxacin	3,47
	Doxycycline	0,28
	Flumequine	0,01
	Sulfamethoxazole	0,03
	Sulfapyridin	0,46
	Trimethoprim	0,8
Antidepressant	Citalopram	2,4
	Escitalopram	2
	Venlafaxine	0,02
	Sertraline	0,03
Antihypertensive	Indapamide	0,03
	Irbesartan	0,03
	Losartan	0,05